AD-A102 889 ROCKWELL INTERNATIONAL THOUSAND OAKS CA ELECTRONICS--ETC F/6 20/2
EPITAXIAL GROWTH OF GEGAAS.(U)
JUN 81 K T IP, R D FAIRMAN, A A IMMORLICA F44620-76-C-0134
UNCLASSIFIED ERC41002.29FR AFOSR-TR-81-0632 NL

1 OF 2
AD A
102889

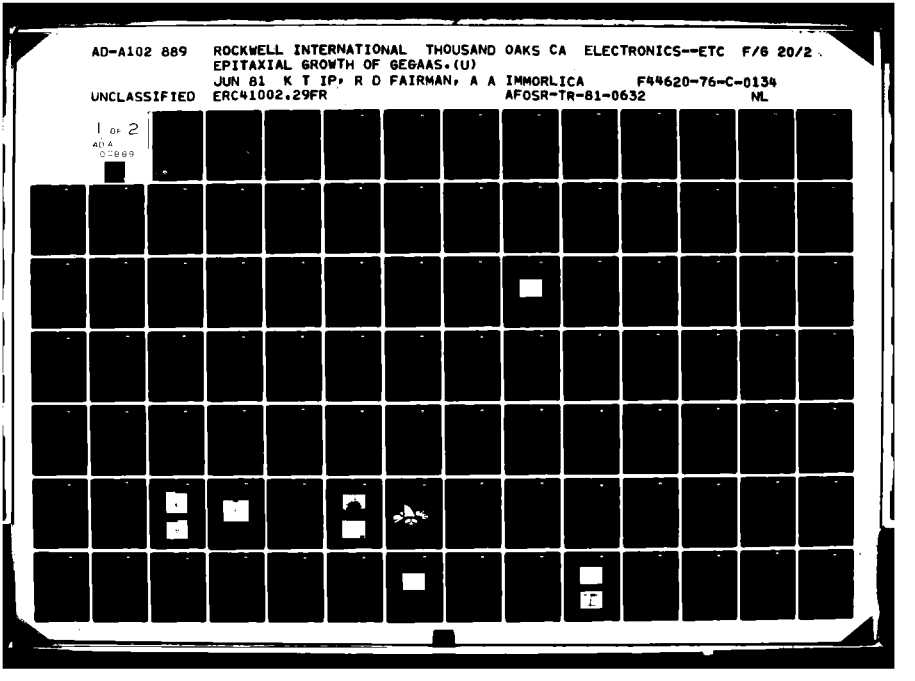

AFOSR-TR-81-0632

ERC41002.29FR

LEVEL II

ERC41002.29FR

Copy No. 16

EPITAXIAL GROWTH OF GeGaAs

FINAL REPORT [redacted]
June 1, 1977 through July 31, 1980

CONTRACT NO. F44620-76-C-0134

Prepared for

Air Force Office of Scientific Research
Electronic & Solid State Sciences
Building 410
Bolling AFB, Washington, DC 20332

R. D. Fairman
A. Immorlica, Jr.
Principal Investigators

JUN [redacted] 1981

Approved for public release; distribution unlimited

Rockwell International
Electronics Research Center

81 8 14 069

UNCLASSIFIED

SECURITY CLASSIFICATION OF THIS PAGE (When Data Entered)

REPORT DOCUMENTATION PAGE	READ INSTRUCTIONS BEFORE COMPLETING FORM
1. REPORT NUMBER **AFOSR-TR- 81 -0632** 2. GOVT ACCESSION NO. AD-A102 899	3. RECIPIENT'S CATALOG NUMBER
4. TITLE (and Subtitle) Epitaxial Growth of GeGaAs	5. TYPE OF REPORT & PERIOD COVERED Final Report 06/01/77 through 07/31/80
	6. PERFORMING ORG. REPORT NUMBER ERC41002.29FR
7. AUTHOR(s) K.T. Ip, R.D. Fairman, A.A. Immorlica, Jr., and B. Ludington	8. CONTRACT OR GRANT NUMBER(s) F44620-76-C-0134
9. PERFORMING ORGANIZATION NAME AND ADDRESS Rockwell International Electronics Research Center 1049 Camino Dos Rios Thousand Oaks, CA 91360	10. PROGRAM ELEMENT, PROJECT, TASK AREA & WORK UNIT NUMBERS 61102F 2306/B1
11. CONTROLLING OFFICE NAME AND ADDRESS Air Force Office of Scientific Research Electronic & Solid State Sciences, Bldg. 410 Bolling AFB, Washington, DC 20332	12. REPORT DATE June 1981
	13. NUMBER OF PAGES 99
14. MONITORING AGENCY NAME & ADDRESS (if different from Controlling Office)	15. SECURITY CLASS. (of this report) Unclassified
	15a. DECLASSIFICATION DOWNGRADING SCHEDULE

16. DISTRIBUTION STATEMENT (of this Report)

Approved for public release; distribution unlimited

17. DISTRIBUTION STATEMENT (of the abstract entered in Block 20, if different from Report)

18. SUPPLEMENTARY NOTES

19. KEY WORDS (Continue on reverse side if necessary and identify by block number)

Ge, GaAs, heterojunction, liquid phase epitaxy, LPE, molecular beam epitaxy, MBE, chemical vapor deposition, CVD, plasma-enhanced chemical vapor deposition, PECVD

20. ABSTRACT (Continue on reverse side if necessary and identify by block number)

This final report summarizes the results of a 4-year research effort; the first two years of which were on liquid phase epitaxial and MBE approaches and the last two years were on the plasma-enhanced CVD technique. The primary conclusions of this work are that: for the LPE technique, in spite of careful control of the kinetic factors, the thermodynamic instabilities at the melt-seed interface are dominant at the initiation of growth. This results in dissolution of a few monolayers of GaAs and subsequent autodoping in the Ge

DD FORM 1 JAN 73 1473 EDITION OF 1 NOV 65 IS OBSOLETE

UNCLASSIFIED

SECURITY CLASSIFICATION OF THIS PAGE (When Data Entered)

single crystal. However, the purity of the Ge layers was greatly improved by using the Plasma-Enhanced CVD technique. P-type layers with $p \sim 1 \times 10^{16}$ cm^{-3} and $\mu p \sim 1500$ $cm^2/V\text{-}s$ have been achieved. Mirror smooth layers with sharp interfaces are routinely obtained. Doping with volatile hydride is compatible with the PECVD technique. P-type layers doped with B_2H_6 to up to $p \sim 4 \times 10^{19}$ cm^{-3} has been obtained. In situ growth of multi-layer structures has also been demonstrated.

TABLE OF CONTENTS

LIST OF FIGURES

LIST OF FIGURES

LIST OF FIGURES

LIST OF FIGURES

LIST OF TABLES

PREFACE

This work was conducted in the Microwave Devices Section of the Advanced Electronics Department at the Rockwell International Electronic Research Center, Thousand Oaks, CA. Personnel contributing to this effort include: Dr. Kwan T. Ip and Mr. Robert Fairman (Plasma-Enhanced CVD), Dr. Anthony A. Immorlica, Jr. and Mr. Burt. W. Ludington (Liquid Phase Epitaxy), Drs. David Miller and F. J. Szalkowski (Molecular Beam Epitaxy), Mr. Robert Fairman and Mr. Jeffrey Dreon (Chemical Vapor Deposition), Dr. Alan Harker (SIMS and SPS) and Dr. Cecil Rhodes (TEM). Dr. Herbert Kroemer (consultant), University of California, Santa Barbara, assisted in the interpretation of the heterojunction characteristics.

The Program Manager was Dr. Daniel R, Ch'en. The Principle Investigators were Dr. A. A. Immorlica, Jr., during program Phase I and Mr. R. D. Fairman during program Phase II. This work is sponsored by the Air Force Office of Scientific Research under Contract No. F44620-76-C-0134 and monitored by Dr. Cole Litton of the Air Force Avionics Laboratory, Dayton, Ohio.

1.0 INTRODUCTON

The Ge-GaAs system attracted a great deal of interest in the late 1950's and early 1960's as an experimental vehicle for the study of the physics of heterojunctions. This was due to the fact that the lattice constants of the two materials are so well matched, offering the possibility of a nearly ideal interface. However, materials growth technology lagged far behind the theoretical interest. Recently, renewed attention has been given to the Ge-GaAs system as a result of the advances achieved in the materials growth technologies such as LPE, MBE and CVD. This time though, the Ge-GaAs system emerges not only as a subject of physical study, but also as a possible semiconductor heterojunction pair for use in the design of multilayer microwave structures. Apart from their excellent match in lattice constants which assures a low interface state density, both germanium and gallium aresenide have since been extensively characterized, exhibiting physical constants which are favorable for many microwave device applications. Thus, there exists a potential for improvement of existing devices as well as the development of new device concepts due to the additional flexibility in device design offered by this heterojunction system. One of the primary reasons for failure to exploit this system to date has been the lack of a sufficiently good materials preparation technology in spite of advances made in the growths of ternary and quaternary materials.

The purpose of this program is to directly address the materials problems which have prevented wide application of Ge-GaAs devices in the

past. These include primarily the control of autodoping and diffusion at the junction as well as the nature of the metallurgical interface and the surface morphology. The original approach in this program was the low temperature liquid phase epitaxy. By thoroughly characterizing the thermodynamics and kinetics of melt systems, and utilizing recent advances in LPE growth techniques, it was originally predicted that layers suitable for microwave device applications could be obtained. While excellent surface morphology, sharp metallurgical interfaces, and excellent growth rates have been demonstrated, thin submicron layers required for microwave device applications were still quite highly doped. Alternate approaches such as MBE and plasma-enhanced CVD technique were investigated. MBE grown Ge were also highly doped because of residual As vapor in the growth chamber. Layers grown using the plasma-enhanced CVD technique exhibited substantially lower carrier concentration, mirror smooth surface and very sharp interface. Volatile hydride doping experiments were also performed. The results indicated that in situ growth of multi-layer structure is possible with PECVD.

This final report summarizes the results of a 4-year research effort; the first two years of which were on liquid phase epitaxial and MBE approaches and the last two years were on the plasma-enhanced CVD technique. The primary conclusions of this work are that: for the LPE technique, in spite of careful control of the kinetic factors, the thermodynamic instabilities at the melt - seed interface are dominant at the initiation of growth. This results in dissolution of a few monolayers of GaAs and subsequent autodoping in the Ge single crystal. For the plasma-enhanced CVD technique, it is observed that

there is carrier "pile-up" near the interface. However, fairly pure Ge layer with $p \sim 10^{16}$ cm^{-3} are obtained for thick layers. Doping using volatile hydride is possible in the PECVD system and controlled doping may be needed to compensate for the interface charges.

2.0 REVIEW OF LIQUID PHASE EPITAXIAL GROWTH

This chapter reviews some of the pertinent results that were directly related to the growth of Ge on GaAs using the liquid phase epitaxial technique. A detail summary on the LPE growth can be found in report No. SC5075.26AR.

Liquid phase epitaxy is an attractive growth method for preparation of multilayer Ge-GaAs device structures for microwave applications. Both Ge and GaAs layers can be rapidly grown in situ with LPE techniques. In situ growth is important for heterojunction devices in order to minimize interface defects which can compromise device efficiencies. Due to low vapor pressures involved (e.g., $P_{As} = 10^{-9}$ atm at 700°C),[1] cross contamination in a well designed LPE system is insignificant with respect to in situ growths by traditional VPE methods, favoring the LPE approach for multilayer Ge-GaAs structures. In addition, well-behaved p and n type dopants for both materials have been identified and characterized with the LPE process. These inherent advantages, coupled with a long standing Electronic Research Center background in liquid phase heteroepitaxy, led to the choice of a LPE approach at the initiation of this work.

The keys to successful liquid phase heteroepitaxy lie in the identification of suitable melt systems and the control of growth kinetics to prevent dissolution of the seed crystal due to the nonequilibrium thermodynamic nature of the melt-seed interface at the initiation of growth. Such instabilities can lead to bandgap grading in the case of ternary III-V compounds,

or to autodoping in the case of the Ge-GaAs system. Early LPE growths of Ge on GaAs[2] utilized the Nelson tipping technique[3] in which precise control of the melt supersaturation and initial nucleation density are difficult to achieve. By employing recent advances in state-of-the-art LPE along with low growth temperatures, it was predicted that problems related to autodoping and diffusion could be overcome. In the initial contract period, a horizontal LPE system incorporating a transparent furnace was designed and fabricated. The multicompartment graphite boat contains source-seed recesses for precise control of melt supersaturation, and lies atop a quartz heat exchanger which provides a well controlled vertical temperature gradient. These features are important for controlling the nucleation density to favor growth over dissolution. This system was utilized to measure fundamental thermodynamic constants of Pb-Ge, Pb-GaAs. Pb-Sn-Ge, Pb/Sn-GaAs, Pb-AlGe, Pb-Al-GaAs and Pb-Ga-Ge over a temperature range of 400 to 700°C.

Initially, Pb was chosen as a liquid solvent for epitaxial growth of Ge. Because of the finite solubility of GaAs in Pb (7×10^{-4} atomic fraction at 500°C) relatively fast initial growth rates were required to prevent macroscopic substrate dissolution. While this was found to result in unstable growth fronts and poor morphology on (100) orientations, excellent morphology was obtained on (111)B substrates. Although no evidence of meltback was optically detected at the metallurgical interface, carrier densities of 10^{18} cm^{-3} and higher were measured. Microscopic meltback was suspected, and a technique was introduced at the conclusion of the first year contract period which showed promise of eliminating meltback by driving down the GaAs

solubility in Pb through addition of a third element to the saturated melt. This ternary melt concept continued into the second year contract period and is described below.

2.1 Investigation of Ternary Melts

In liquid phase heteroepitaxial growth, a potential for substrate meltback exists because the seed substrate is not normally in thermodynamic equilibrium with the growth melt. While we have found it possible to prevent macroscopic melt-back by controlling the kinetic growth factors, a microscopic dissolution of even a few monolayers would be enough to degenerately dope a submicron-thick Ge layer. One approach to this problem is the identification of a melt system for which the solubility of GaAs is vanishingly small.

Towards the end of the first year contract period, a new approach to the microscopic melt-back problem was introduced. The melt-back suppression technique involves the addition to the melt a third element to a saturated melt which functions to suppress the solubility of GaAs. Ideally, the element should occupy a neutral site in the Ge lattice or, alternatively, be effective at such low concentrations that the carrier density in the Ge layer remains below a certain desired value. It was demonstrated that the addition of Al to the Pb melt has a remarkable effect on the solubility of GaAs over the temperature range employed for liquid phase epitaxy. No solubility of GaAs in Pb could be detected for additions of Al to the melt at a concentration of about 10^{-3} atomic fraction. Unfortunately, Al is a shallow acceptor in Ge. Thus, a series of growths was initiated in order to determine if even smaller

amounts of Al would be effective in reducing microscopic dissolution without appreciably doping the Ge p-type due to the addition of Al to the melt.

Figure 2.1 shows the net carrier density of the Ge layers as a function of the mole-fraction of Al added to the saturated Pb-Ge melt. The carrier density was determined by Van der Paw measurements. The letter next to each data point indicates the conductivity type of that particular layer. Layers having Al atom fractions in the melt greater than 2×10^{-5} were all p-type as expected. The carrier density falls rapidly with Al atomic fraction down to approximately 5×10^{-5} below which the carrier density levels off and begins to increase. Considerable spread is seen for the lower Al concentrations, and the conductivity fluctuates from p- to n-type. Thus, it appears at concentrations below about 5×10^{-5} that the Al becomes ineffective at suppressing the solubility of GaAs in the melt and that the carrier density seen at these low Al concentrations are due to microscopic dissolution at the initiation of growth. Thus, the success of the melts suppression concept relies on the identification of another element which suppresses the solubility of GaAs in Pb and, in addition, occupies a neutral site in the Ge lattice. The identification of such an element will require futher fundamental solubility measurements.

2.1.1 Dependence on Growth Temperature

Another source of autodoping in epitaxial growth is mutual solid-state diffusion at the growth temperature. For the liquid phase growths of Ge on GaAs at 575°C, it is unlikely that the high carrier densities reported in

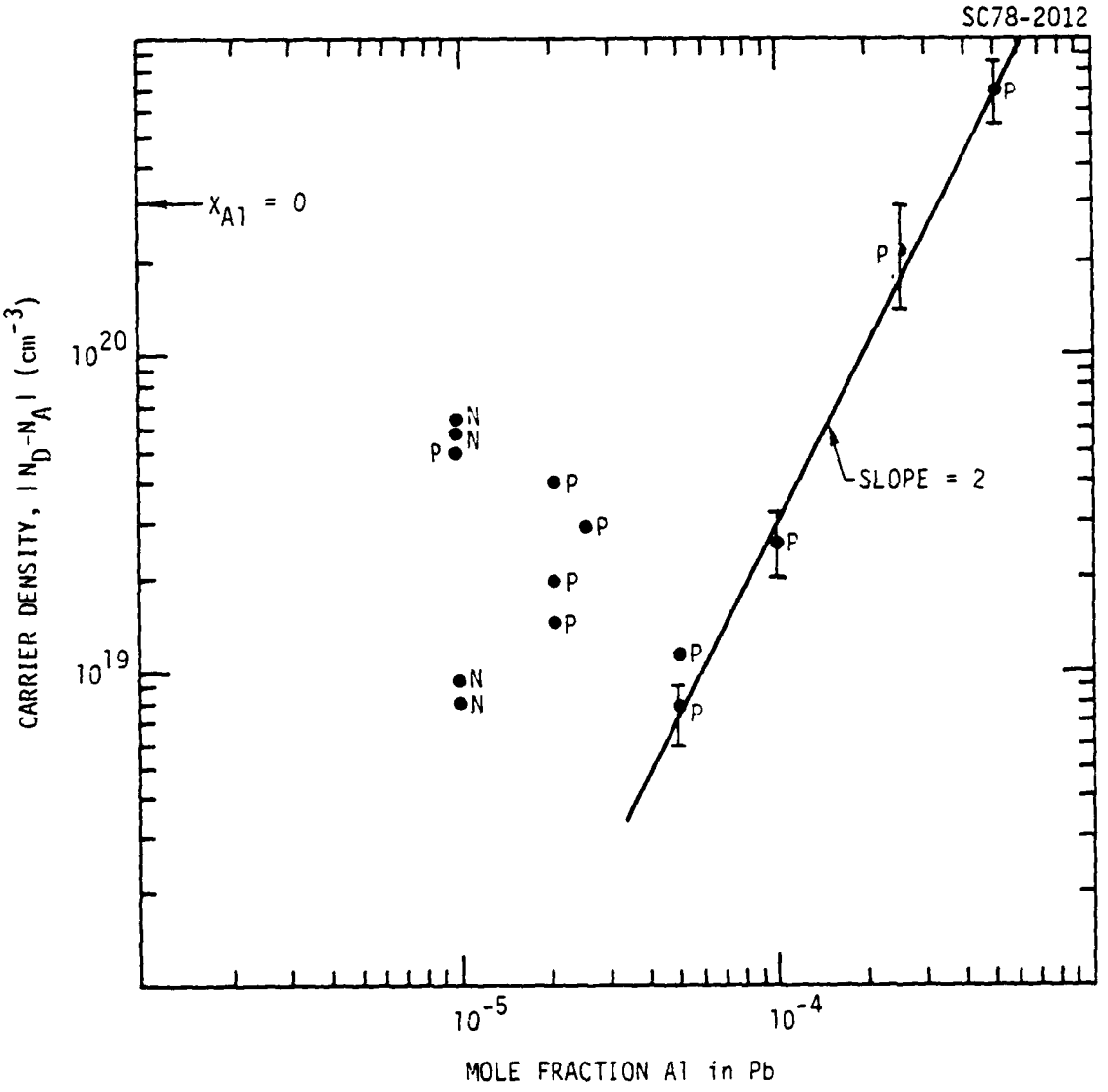

Fig. 2.1 Net carrier density vs mole fraction of Al in Pb melt. Conductivity type is noted next to each datum point.

the last section are due to diffusion. This is due to the fact that the growths occur over a relatively short time (typically less than 5 min) after which the furnace is rapidly quenched. The diffusivities of As and Ga in Ge at 575°C are 9.5×10^{-15} and 1.3×10^{-17} cm^2/s, respectively,[4] resulting in diffusion lengths of only 170 and 6 Å, respectively, for t = 300 s. Nevertheless, it is desirable to reduce the growth temprature to minimize lattice strain due to the differential thermal expansion coefficients of Ge and GaAs. Thus, a series of growths was undertaken in order to determine the lower temperature limit at which one can still obtain continuous epitaxial layers with good surface morphology.

Continuous Ge epitaxial layers were nucleated from Pb solutions at temperatures as low as 450°C. Both crystal orientation and vertical temperature gradient were found to be important parameters in obtaining smooth morphologies. Below this temperature, island growth is observed and the layers tend to be discontinuous. This may be due to the lowered solubility of Ge in Pb at these temperatures. In order to further reduce the growth temperarure, an eutectic mixture of Pb and Sn was used as a melt.

The solubility of Ge in a PbSn eutetic mixture is significantly higher than the solubility of Ge in pure Pb. This shown in Table 2.1 which is a tabulation of data taken from measured solubilities reported previously. Although the GaAs solubility is higher in the mixture as well, the ratio of Ge to GaAs solubilities has also increased by a factor of two, yielding a more favorable driving force for nucleation over substrate dissolution.

Table 2.1

Solubilities of Ge and GaAs in Pb and Pb/Sn at 450°C

	Pure Pb	Eutectic Pb/Sn
Ge Solubility, X_{Ge}	2.2×10^{-3}	3.5×10^{-2}
GaAs Solubility, X_{GaAs}	3.6×10^{-4}	2.8×10^{-3}
Ratio X_{Ge}/X_{GaAs}	6.1	12.5

Ge was grown from a saturated PbSn eutectic mixture on (111)A GaAs substrates at a supercooling approaching 50°C. Nucleation at the 425°C contact temperature was nearly instantaneous as judged by the complete coverage of the GaAs substrate after momentary contact of approximately 1 s. This was in marked contrast to growth from pure Pb in which the Ge nucleated at isolated sites before coalescing into a planar layer after several seconds of growth. Surface morphology was quite dependent on the amount of supercooling, with 12-14°C being most optimum. The carrier density of these layers was typically about five times lower than for layers nucleated from Pb melts at slightly higher temperatures. This is attributed to the faster nucleation time and larger Ge/GaAs solubility ratios in the Pb/Sn melt system. Based on the Ge solubility in Pb/Sn, continuous layers should be obtainable at temperatures approaching 350°C provided that the Ge atom surface mobility remains adequate.

During the series of growths from Pb melts an interesting phenomena was observed with regard to the conductivity of the grown layers. Layers grown above 575°C were primarily p-type, while those below this growth temper-

ature were all n-type. The former conductivity is ascribed to Ga doping, while the latter is ascribed to As doping. The fact that a transition from p- to n-type was observed with lower growth temperatures, suggests that the Ga and As distribution coefficients are equal at some point in this temperature interval, with As having a higher distribution coefficient at the lower temperatures. Presuming a well defined transition from n- to p-type exists, one might be able to grow layers at this temperature, yielding self-compensating shallow donor acceptor levels. Addition of a deep level to the crystal lattice at this point would further pin the fermi level near mid-gap, resulting in high resistivity epitaxial material. These thoughts lead to a parallel investigation of compensation effects in epitaxially grown Ge; these are discussed in the following section.

2.1.2 Compensation, Ion Bombardment and Annealing

As discussed above, the appearance of a n-p transition with growth temperature encouraged the investigation of compensation effects. Three approaches were considered: melt doping with a deep-level impurity, solid-state diffusion, and ion implantation. Tellurium, Ni, and Se were chosen for use in these studies.

The use of Te was investigated for compensation of shallow acceptors in the Ge epitaxial layers grown above the transition temperature. Tellurium is reportedly a deep donor in Ge with levels at 0.11 and 0.30 eV.[5] Solubility measurements at 575°C revealed that the addition of 1 at% Te has no effect on the Ge or GaAs solubilities in Pb, as would be expected for regular solutions.

Germanium layers were grown from Pb melts having 0.012 to 1.0% Te. No significant effect of the carrier density was noted and the mobility remained characteristic of layers grown at these temperatures. These results may be due to a low distribution coefficient of Te in Ge when grown from Pb. While little relevant data for distribution coefficients for low temperature LPE Ge growths could be found in the literature, a distribution coefficient of Te in melt-grown Ge of 10^{-6} has been reported,[6] suggesting that little Te would have been incorporated in the Ge LPE crystal. Thus, due to the low distribution coefficients as well as low solubilities of other deep levels in liquid Pb at these growth temperatures, solid-state diffusion, rather than melt doping, was next investigated.

Nickel is an interesting deep level acceptor in Ge, particularly due to the fact that it exhibits a relatively high temperature independent diffusion coefficient of 4.5×10^{-5} cm^2/s.[4] Although its solid solubility is quite low, some initial experiments were carried out with Ni in order to determine if it would be useful for compensating Ge layers at the transition temperature. Nickel was evaporated on Ge substrates and diffused at 500°C for 15 min in a forming gas atmosphere. After diffusion, the Ni was removed by placing the sample under liquid Ga in an HCl solution. The electrical characteristics before and after diffusion were measured by the Van der Pauw technique and are given in Table 2.2. As shown, the net donor concentration dropped to the near intrinsic value as expected, while the mobility showed a sharp increase. The latter behavior was surprising since it was expected that the compensated sample would result in presence of additional scattering sites

which would degrade the mobility rather than improve it. It could be that the short-term heat treatment is responsible for the improved mobility due to the annealing of lattice defects. An n-type epitaxial layer grown at 575°C, was also diffused with Ni in the same manner. As expected, there was no significant change in the net donor concentration due to the fact that the solubility of Ni is significantly less than the shallow donor levels. However, a significant drop in mobility was observed, suggesting that the Ni is playing an important role in the scattering mechanisms in the layer. It is felt that Ni can be a useful deep level impurity provided that a growth temperature can be found such that the shallow donor and acceptor levels are somewhat self-compensating.

Table 2.2

Characteristics of Ni Diffused Ge

	Net Donor Concentration (cm^{-3})	Mobility (cm^2/v-s)
Single Crystal Ge Substrate		
Before Ni diffusion	8.4×10^{13}	2560
After Ni diffusion (500°C, 15 min)	2.5×10^{13}	4325
Epitaxial Layer 77F10		
As grown (@ 575°C)	7.7×10^{18}	210
After Ni diffusion (500°C, 15 min)	7.6×10^{18}	162

Another technique which was considered for compensation was the introduction of a deep level via ion implantation. Selenium, a donor level in

Ge with levels at 0.14 and 0.26 eV,[5] was chosen for this study and implanted at 500 keV at a dose of 1×10^{14} cm^{-2}. The projected range and standard deviation of 500 keV Se in Ge is estimated to be 1700 Å and 670 Å, respectively, giving a peak atomic concentration of 6×10^{19} cm^{-3}. Selenium was implanted into single-crystal Ge substrates which were measured both before and after a 1-hr anneal at 575°C. Results shown in Table 2.3 indicate that some annealing occurs at room temperatures. Measurements were taken both 3 and 13 days after implantation as well as after a 1-hr anneal at 575°C. A monotonically increasing carrier concentration from 8.4×10^{13} to 1.2×10^{15} with a corresponding decrease in the carrier mobility is seen. Characteristics of a p-type epitaxial layer (grown at 575°C) as a function of annealing and implantation are also shown in Table 2.3. Anneal time and temperature were chosen to be 575°C in 1 hr, respectively. Considering the diffusivities of As and Ga under these conditions, the resulting diffusion lengths, 580 Å and 20 Å, would not be expected to significantly alter the carrier density in the epitaxial layer due to diffusion from the GaAs substrate. After a 1-hr anneal of the as-grown layer, a decrease in the net acceptor concentration from 9.9 to 6.9×10^{18} cm^{-3} was observed with a corresponding increase in Hall mobility. This may indicate an annealing of electrically active defects in the grown epitaxial layer which might partially account for the high carrier densities normally observed in these layers. After Se implantation but before anneal, the net acceptor concentration decrease was accompanied by an increase in mobility. While a drop in carrier density would be expected due to radiation damage, the mobility increase is unexplained. After annealing of the

implanted sample, however, the net hole concentration increased past the original acceptor level in the grown crystal, contrary to the expected effect. At this time, no conclusion can be drawn from these behaviors without further investigation. The work was undertaken in anticipation of locating a transition temperature in the epitaxial growth process. However, because a well defined transition was not found, it was decided to curtail the work on compensation effects. Nevertheless, the data presented here can form a basis for further studies if it is determined that such studies are warranted.

Table 2.3

Ge Electrical Characteristics (at 300°K) as a Function of Annealing and Implantation

	Net Carrier Concentration (cm^{-3})	Mobility (cm^2/v-s)	Conductivity Type
Single Crystal Ge Substrate			
Before implant	8.4×10^{13}	2560	n
3 days after Se implant	3.6×10^{14}	822	n
13 days after Se implant	8.4×10^{14}	325	n
After 1-hr anneal (@ 575°C)	1.2×10^{15}	261	n
Epitaxial Layer 56F10			
As Grown (@ 575°C)	9.9×10^{18}	72	p
After 1-hr anneal (@ 575°C)	6.9×10^{18}	185	p
After Se implant (500 keV, 1×10^{14} cm^{-2})	3.2×10^{18}	555	p
After implant and anneal (575°C, 1 hr)	1.4×10^{19}	169	p

2.2 Characterization of LPE Grown Layers

2.2.1 Chemical Analysis

Several analytical techniques are available to assess the chemical nature of the epitaxial layers. For thin-film analyses, secondary ion mass spectrometry (SIMS), x-ray photoelectron spectrometry (XPS), nondispersive x-ray analysis, and Auger spectroscopy are available. XPS and Auger techniques yield quantitative information about the chemical bonding and nature of a surface, but have limited sensitivities of about 0.1%. For a straightforward chemical analysis, SIMS is preferred as atomic concentrations of 10^{17} to 10^{18} cm^{-3} can be detected. Because SIMS is a semiquantitative technique, it is often employed in conjunction with XPS. The atomic profile of a thin layer can also be determined using SIMS, XPS or Auger by in situ sputtering, which is, of course, inherent in the SIMS technique. Nondispersive x-ray energy analysis in a scanning electron microscope can also be employed, as it was earlier in this work, to investigate the abruptness of an interface by probing a cleaved edge. However, in most materials, an x-ray yield can be detected from a region which is a sizeable fraction of a micron, even though a beam diameter of only several hundred angstroms is employed.[7] From measurements on initial layers it was concluded that the interface was more abrupt than the resolution of the probe. Thus, this latter technique was abandoned in favor of SIMS profiling which is reported below.

Secondary ion mass spectroscopy (SIMS) was used in conjunction with x-ray photoelectron spectroscopy (XPS) to obtain a chemical profile through

the Ge-GaAs interface. These measurements were carried out at the Science Center using a recently acquired 3M, Inc., SIMS gun. The sputtering was accomplished with a rastered Ar-ion beam while the detector was gated in order to minimize contributions from the sidewalls of the etched hole.

Survey spectra were taken from 0 to 100 atom mass units (amu) both before and after Ar ion sputtering through the Ge-GaAs interface. These spectra are shown in Fig. 2.2 and 2.3 for layer 112F10. Only positive ions were monitored and, thus, As does not appear in these analyses. The prominent Na and K peaks are due to sample surface and chamber contamination and are commonly seen in these spectra, particularly because of the high relative sensitivity of these ions (see Table 2.4). The presence of Al is attributed to residual Al_2O_3 polishing compound which was used to mechanically thin the layer prior to analysis; microscopic examination of the surface after analysis revealed the presence of particulate matter on the sample. Other impurities identified in the 0-100 amu scan of the Ge surface include Mg and Ca, which were present in the Pb analyses, and Si which is probably introduced in the growth process. The five Ge isotopes are seen in the initial scan while the two Ga isotopes clearly appear in the post sputtering spectra.

The Ga signals are considerably stronger than the Ge due to the higher sensitivity of the former. The ratio of sensitivities was calculated by comparing the SIMS signal peaks to the XPS signals with the result that Ga sensitivity is ~ 24 times greater than Ge. For comparison, the relative sensitivities of all elements detected in the analysis are given in Table 2.4.

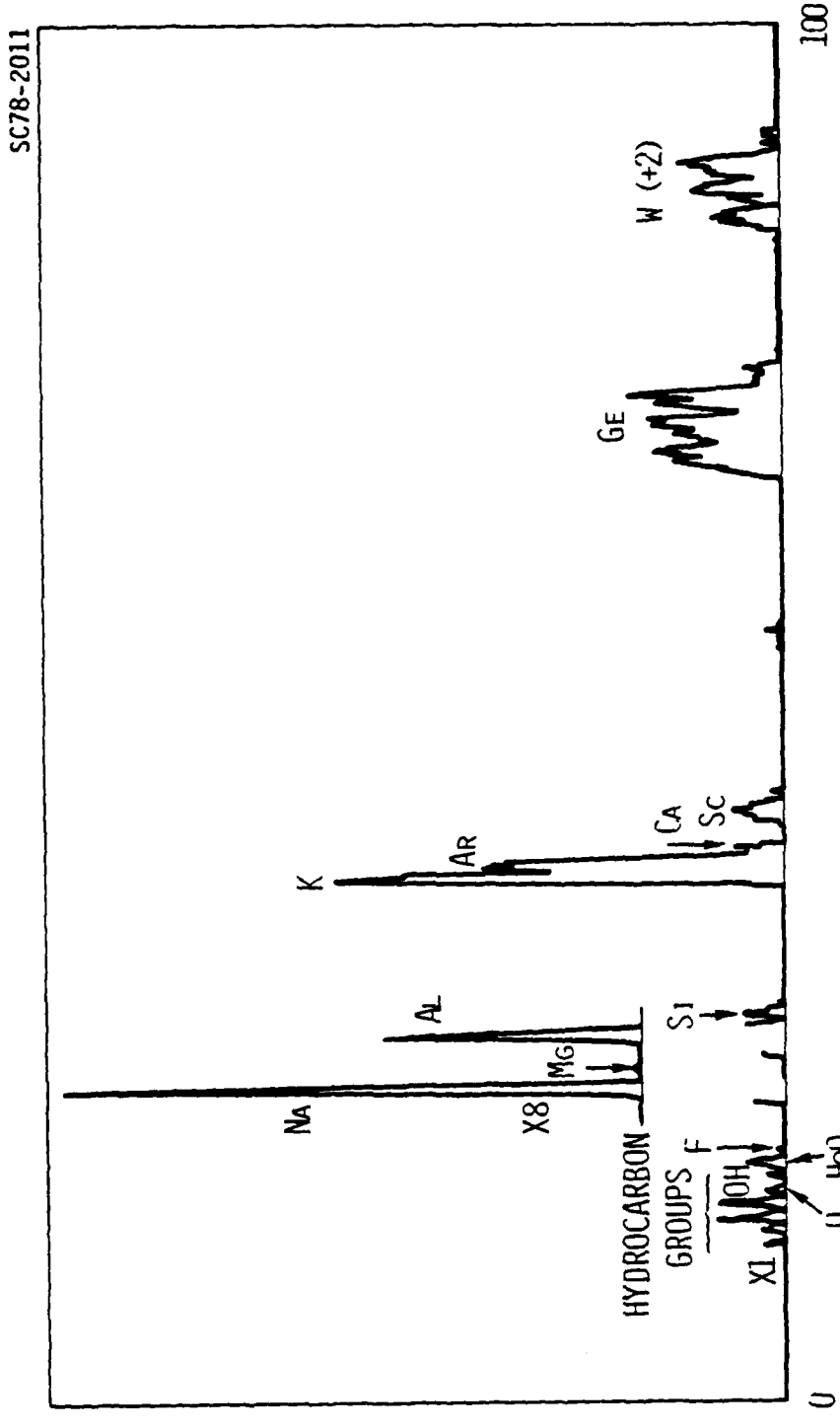

Fig. 2.2 Survey SIMS scan of an epitaxial Ge surface.

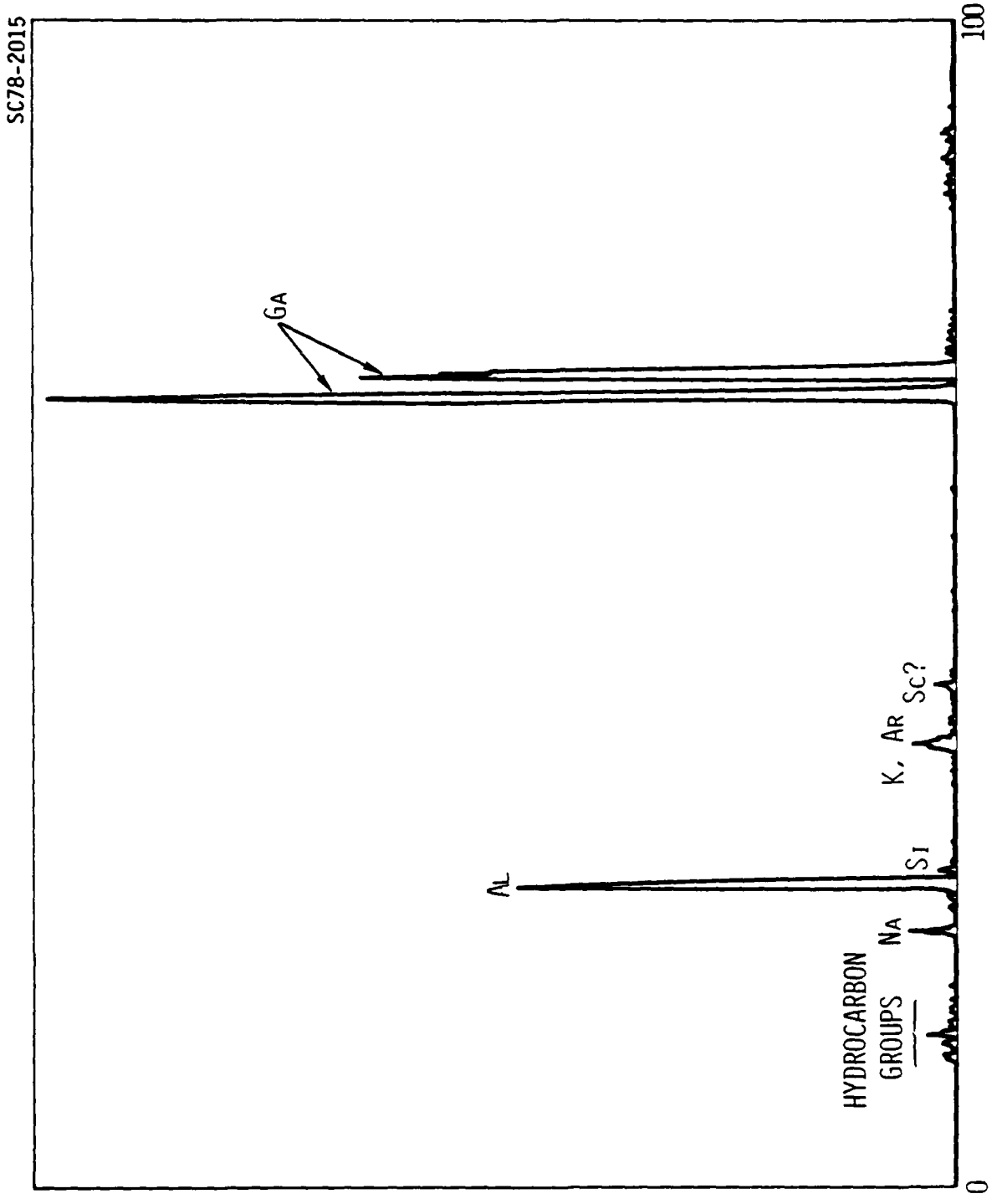

Fig. 2.3 Survey SIMS scan of GaAs substrate after sputter removal of the Ge epitaxial layer.

Table 2.4

Relative Ion Yield of Selected Elements Detected by SIMS

Element	Relative Yield
C	26
O	10
F	4
Na	2400
Mg	260
Al	200
Si	44
K	2100
Ca	400
Ge	7
Ga	170

Profiles of Ge and Ga through the heterojunction interface are shown in Fig. 2.4. This layer was grown from a Pb/Sn melt at 450°C and has an n-type carrier density of 7×10^{18} cm^{-3}. The profiles were taken by monitoring the 73.9 amu Ge and 68.9 amu Ga isotopes as a function of sputtering time during two separate runs. The depth scale was determined by measuring the etched hole with a moving stylus depth indicator and calculating an average etch rate which was assumed equal for both Ge and GaAs.

The Ge interface is seen to be quite abrupt, having a measured transition in this case of about 200 Å. This should be viewed as an upper limit, as the sputtering process does tend to roughen the surfaces causing some convolution of the actual profile. The Ga profile, however, is quite

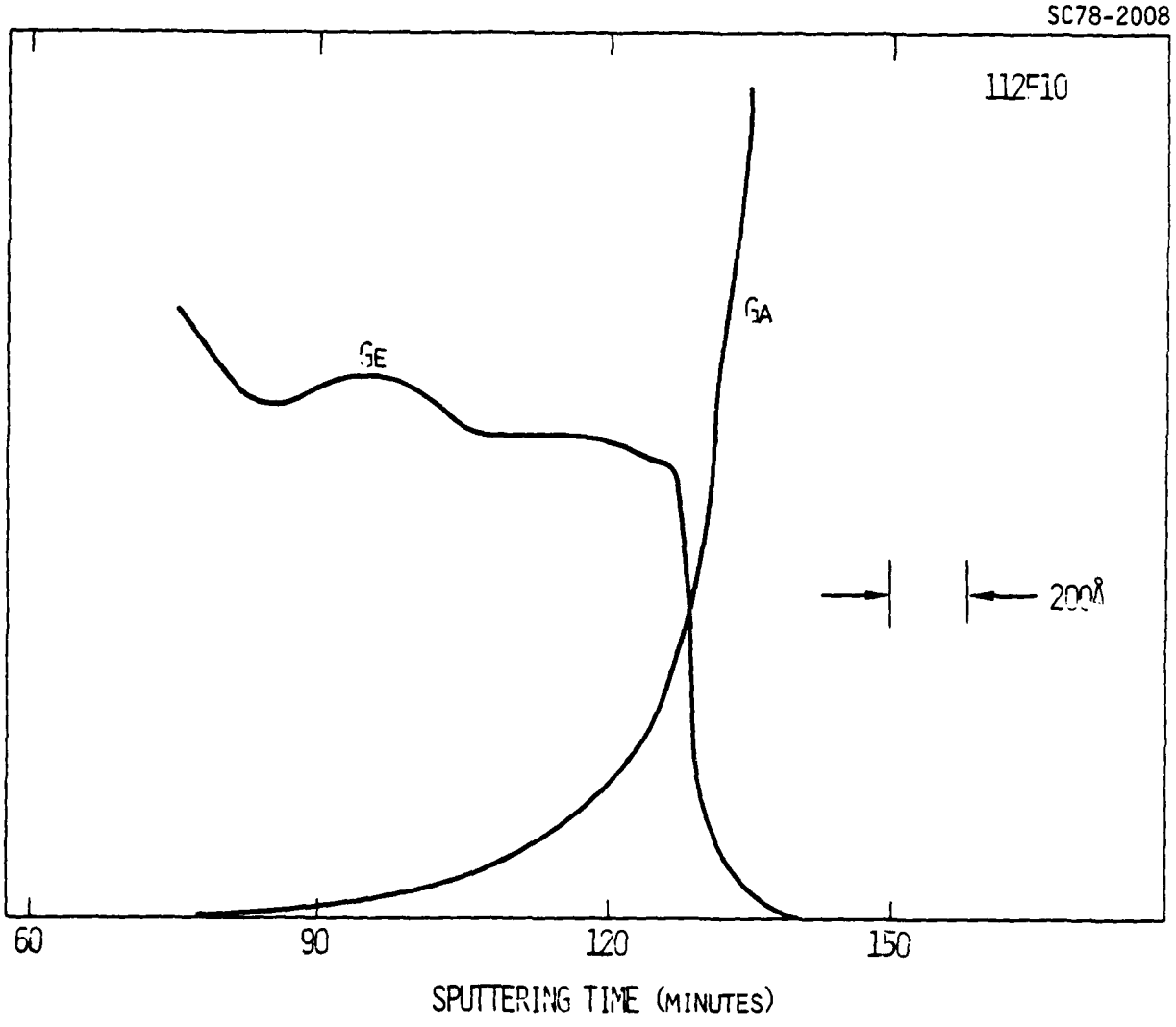

Fig. 2.4 SIMS profile through a Ge-GaAs heterojunction grown from an eutectic Pb/Sn melt. The survey scans before and after sputtering are shown in Figs. 2.2 and 2.3.

broad in comparison. It exhibits a ~ 1000 Å transition from the interface into the noise level, clearly illustrating the effect of microscopic dissolution and autodoping of the Ge layer. It is assumed that the As profile exhibits similar broadening.

A layer grown from a Pb melt was also profiled with results shown in Fig. 2.5. For this case, the measured Ge transition is considerably broader with respect to the layer grown from a Pb/Sn melt. It is felt, however, that this apparent broadening is due to a nonplanar interface on a microscopic level. Thus, both Ge and GaAs crystallites would be contributing to the SIMS signal. Presuming the actual transition is on the order of 200 Å, as measured for the previous sample, an average crystallite thickness of 400 Å is calculated from the differences in the measured transition width of the Ge. It is presumed that the layer first nucleates at isolated sites before coalescing into a continuous layer. During this nucleation interval, the exposed GaAs is available for etchback. This time interval is a function of growth parameters and can be judged by retracting the melt from the seed substrate after momentary contact. The time for nucleating a continuous layer has been observed to be as long as several seconds for growths from Pb melts, while being a fraction of a second for supercooled Pb/Sn melts. The faster nucleation time for Pb/Sn melts is also supported by the fact that the carrier densities in layers grown from Pb/Sn were generally 5X lower.

From these analyses, it is concluded that the LPE grown Ge-GaAs heterojunctions exhibit an interface broadening of less than 40 atomic layers when grown from a Ge saturated Pb/Sn eutectic melt. The high carrier

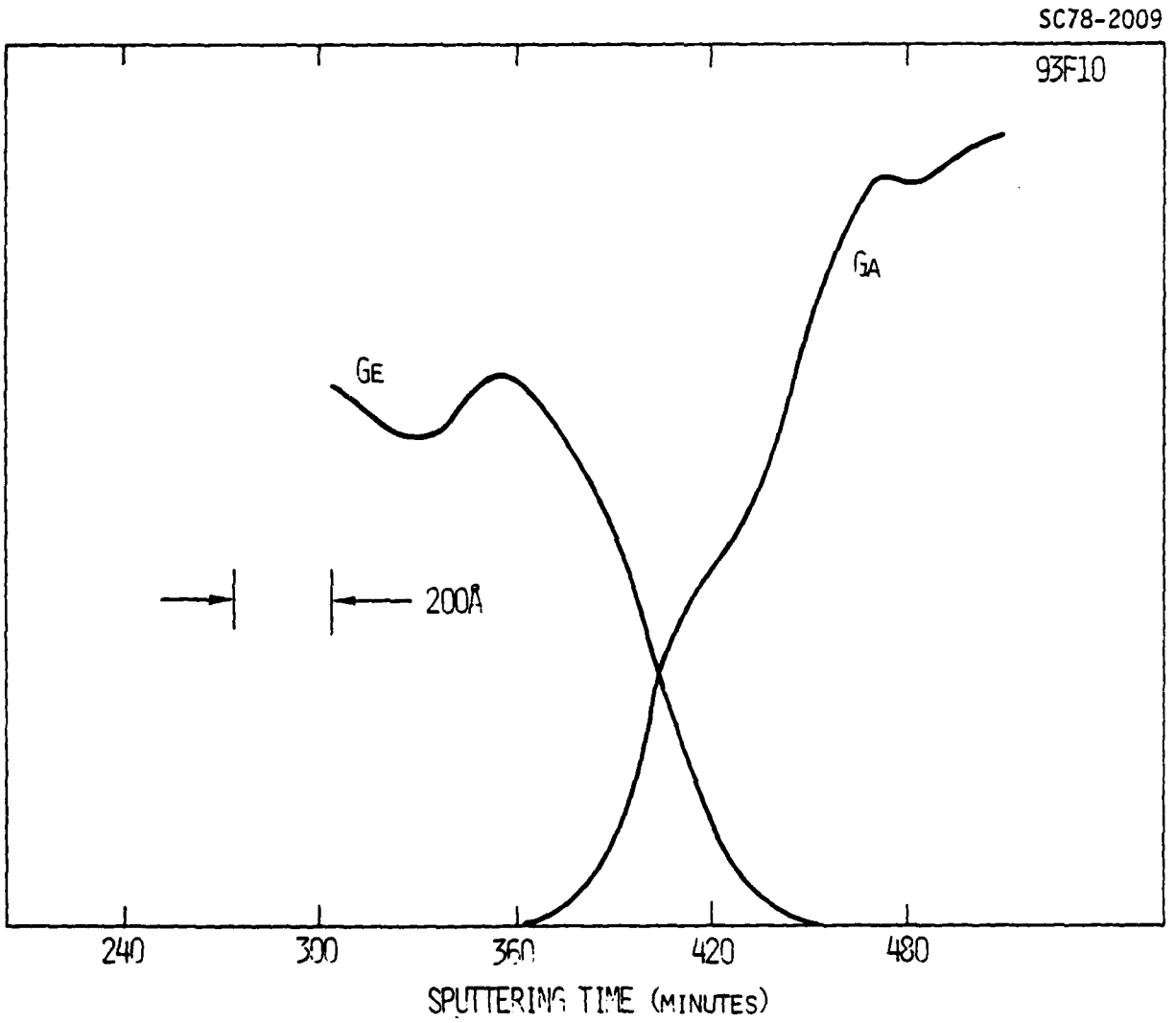

Fig. 2.5 SIMS profile through a Ge-GaAs heterojunction grown from a Pb melt.

densities observed in the layers are undoubtedly a result of microscopic dissolution of the GaAs substrate prior to the nucleation of a continuous Ge layer. While the minimum obtainable carrier density has not yet been established, particularly for submicron thick layers, it is clear that choice of a melt system is a key to minimizing the autodoping effects.

2.2.2 Electrical Measurements

2.2.2.1 PN Junctions

In order to assess the electrical nature of the heterojunction interface, LPE grown Ge-GaAs p^+n heterojunctions are being fabricated and initial results are reported here. Gallium-arsenide and Ge epitaxial layers are grown at 700°C and 450°C, respectively. The GaAs layers are grown from an undoped Ga melt while the Ge layers are grown from an eutectic Pb-Sn melt with about 5 wt% Ga added for intentional p-type doping. A (111) n^+ GaAs Si-doped substrate is used. Titanium-gold contacts were defined on the Ge surface by standard photolithographic lifting techniques after which Ge mesas are etched with a H_2O_2 solution at 40°C. This etch selectively removes Ge at a rate of approximately 500 A/min; no etching of the GaAs could be detected.

The I-V characteristics of a p^+n heterojunction are shown in Fig. 2.6. The n-type GaAs layer was grown in a separate system and has a carrier density of 1×10^{16} cm^{-3}. The reverse current voltage characteristics exhibit some "looping" at low current levels which is not observed for in situ grown junctions and may be due to interface states. A log-linear plot of the

SC78-2016

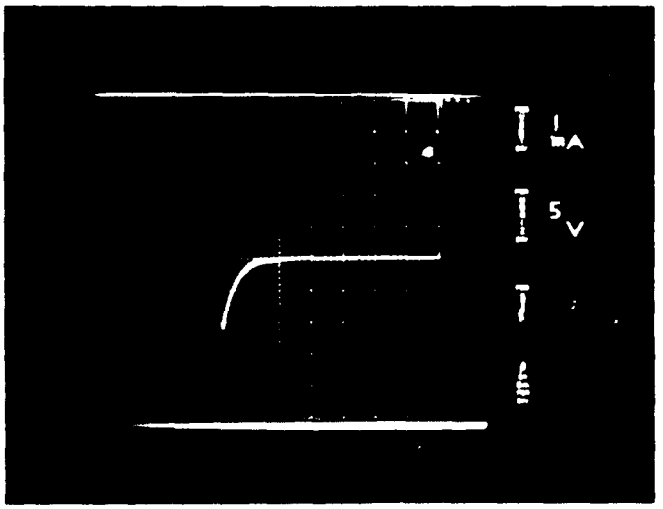

Fig. 2.6 I-V characteristics of a Ge-GaAs p^+-n heterojunction (117F10).

forward I-V characteristic of an in situ grown junction, Fig. 2.7, shows a linear behavior over 6 orders of magnitude of current with an ideality factor of 1.19. The ideality factor, n, is defined by the equation:

$$I = I_0 \exp [q(V-IR)/nkT] - 1 \qquad (2.1)$$

where V is the applied voltage, R is the series resistance, q is the electronic charge, T is the kelvin temperature, k is the Boltzman constant, I_0 is the saturation current, and I is the terminal diode currant. The well behaved linear I-V characteristics shown in Fig. 2.7 are typical of the LPE heterojunction devices which were grown in situ. Diodes for which the GaAs layer was grown in a separate furnace were not well behaved exhibiting an anomalously high ideality factor as well as a weak temperature dependence. This confirms that in situ grown of p-n heterojunctions is important in order to obtain a well behaved device characteristic.

Capacitance-voltage data taken on a heterojunction diode is shown in Fig. 2.8. These preliminary results show a square law behavior to about -14 V bias, past which the depletion layer punches through to the GaAs substrate. A plot of $1/C^2$ vs V for lower biases yields a voltage intercept of 1.0 V.

2.2.2.2 Van der Pauw Data

Hall effect data was taken by the Van der Pauw method on most of the grown layers as well as the Ge source material in order to determine carrier density, mobility, and conductivity type. Typical values obtained on layers

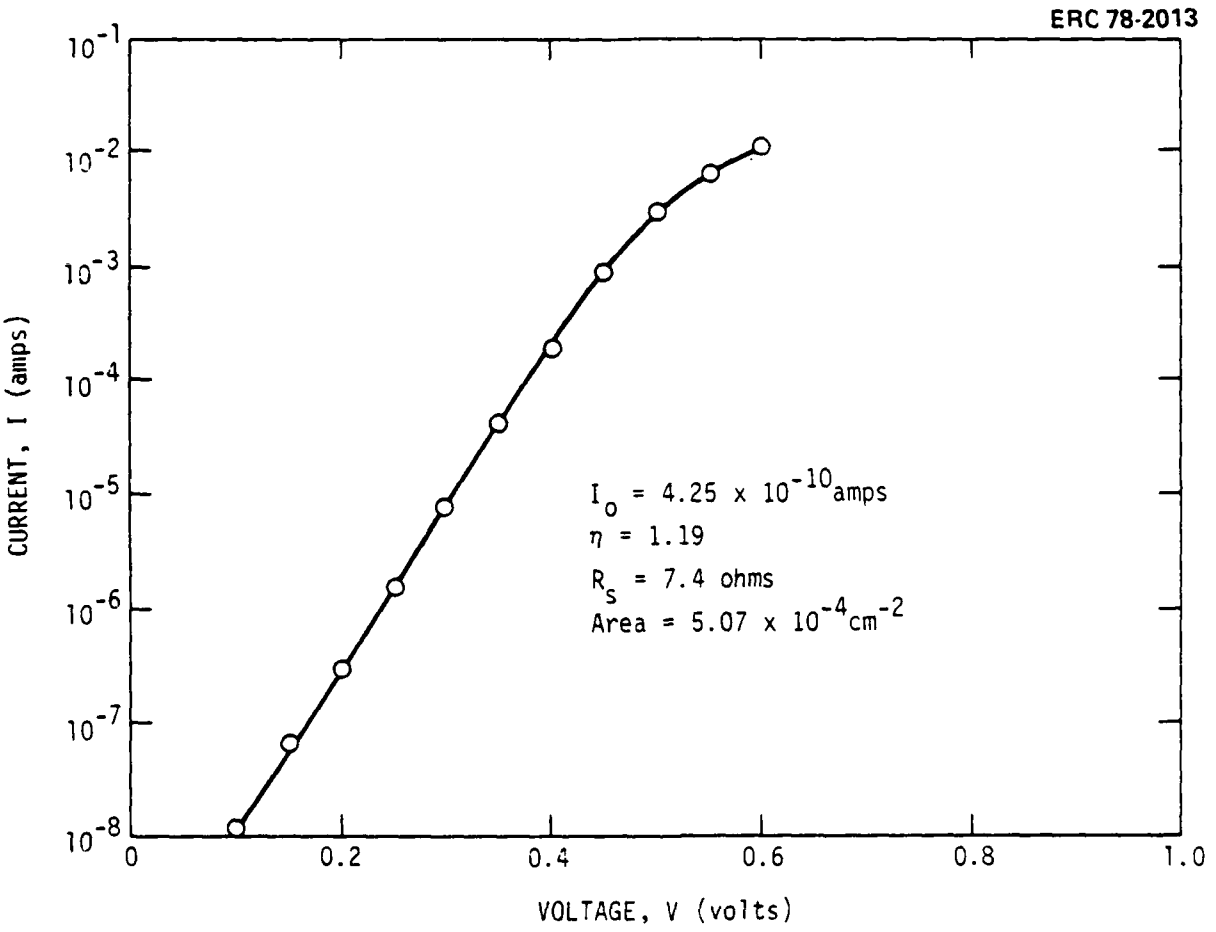

Fig. 2.7 Log-linear plot of the forward current-voltage characteristics of an in situ grown p^+n heterojunction. The solid line is a least square fit to Eq. (2.1).

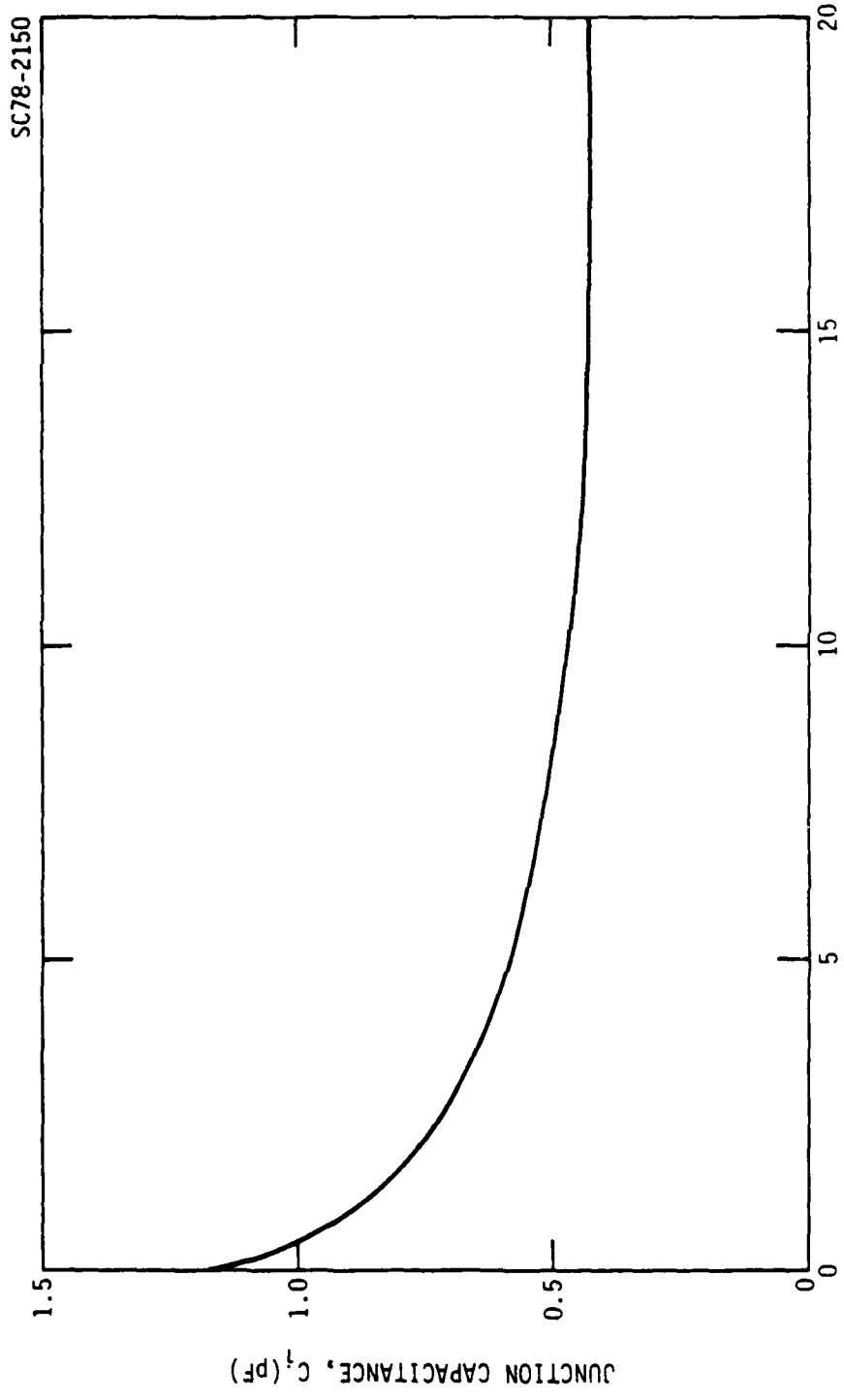

Fig. 2.8 Measured capacitance-voltage characteristic of a Ge-GaAs p^+n junction.

grown from Pb and Pb/Sn melts are shown in Table 2.5. The thickness of the layers ranged from 0.3 to 2 μm. The carrier mobility was higher for growths from Pb melts while the carrier density lower for the Pb-Sn melt growths. This latter factor is undoubtedly due to the fact that nucleation time for growths from Pb/Sn is significantly lower than the nucleation time for growth from Pb. The lower mobility for the Pb/Sn case probably rises from the fact that Sn is incorporated into the lattice and acts as a neutral scattering site.

Table 2.5

Typical Hall Data for Ge Layers and Source Materials

	Net Carrier Density (cm^{-3})	Mobility (cm^2/v-s)
Growths from Pb	4×10^{19}	150
Growths from Pb/Sn	7.6×10^{18}	80
Single crystal substrates	8.4×10^{13}	2560

2.3 Discussion

2.3.1 Liquid Phase Epitaxy

The low temperature liquid phase epitaxial techniques developed in this study have resulted in the controlled growth of submicron thick Ge layers having smooth surface morphologies and sharp metallurgical interfaces. However, in spite of control of kinetic factors governing nucleation, highly

doped layers have resulted. A number of factors can contribute to this: purity of starting materials, rapid diffusion of impurities from the Cr-doped substrate, solid-state diffusion of Ga or As, structural defects in epitaxial layer and autodoping via substrate dissolution. The Ge source material was cut from an undoped, boat grown ingot having a background carrier density of less than 1×10^{14} cm^{-3}. No troublesome shallow impurites were detected at sufficiently high levels by either emission or mass spectroscopy to account for the high carrier densities. Extended baking of the melts in H_2 prior to growth did not result in a consistent decrease in the carrier density level in the Ge epitaxial layer as it is observed for extended Ga bakes in growth of GaAs. Diffusion of impurities from the Cr-doped substrate (primarily utilized in this study to facilitate Hall effect measurements) was also ruled out by growing on in situ GaAs epitaxial layers and sampling substrates from different boules including Si and Zn doped material. While the later exercise did not affect layer purity, it did demonstrate the importance of crystal orientation. Substrates from one boule, misorientated by 2.4°, resulted in growth hillocks on nominal (111)B face. Diffusion of Ga and As from the GaAs would not be expected to be a factor affecting layer purity due to the low growth temperatures and relatively fast growth rates employed. There is some evidence that structural defects may be a cause for concern, as a subsequent anneal of an epitaxial layer grown at 575°C resulted in a significant increase in carrier mobility, possibly due to an annealing of defects. However, further measurements need to be done to confirm this as other factors may be responsible for the increased mobility. It appears, at present, that

autodoping via microscopic substrate dissolution is the most probable factor affecting layer purity.

Base on the electrical and chemical analysis of the grown layers, thermodynamic instabilities in the Ge LPE growth from Pb and Pb/Sn solvents thus appear to be sufficiently high to etchback some tens of monolayers, which is sufficient to autodope submicron thick layers. Such etchback is not unique to the Ge-GaAs system, as bandgap transition regions on the order of 100 Å are observed in the AlAs-GaAs system, for example.[8] Thus, a more ideal melt system, one in which the GaAs solubility is lower with respect to the Ge solubility, or ideally, one in which GaAs is immiscible, need to be identified. Improved results have been obtained with eutectic Pb/Sn mixtures in which the Ge:GaAs solubility ratio is increased a factor of two with respect to pure Pb melts. Of even greater interest is the ternary melt concept, in which trace amounts of a third element are added to a saturated Pb-Ge mixture resulting in a miscibility gap with GaAs. Such behavior has been observed in the Pb-Ge-Al system as discussed. Aluminum, however, is a shallow acceptor in Ge and thus not suitable for growth of undoped layers. It is clear, then, that a considerable amount of work need be expended in order to identify an ideal melt system. Alternate approaches have been considered. In the next section some initial results with Molecular Beam Epitaxy are described.

2.3.2 Molecular Beam Epitaxy

MBE is a promising approach for growth of thin semiconductor films which, due to thermodynamic limitations, are difficult to nucleate by liquid or vapor phase epitaxial techniques. Germanium was epitaxially grown on (100) GaAs substrates at various growth rates and substrate temperatures. An MBE system designed and built at the Electronic Research Center and normally used for growth of III-V compounds was employed. Initial growths at substrate temperatures near 500°C yielded highly doped n-type Ge which was thought due to As doping. This was confirmed by XPS measurements of the Ge surface. Large variations of the growth rate in subsequent runs did not substantially effect the electrical results, suggesting that autodoping due to diffusion was not responsible for the high measured carrier densities. The net carrier concentration did, however, fall rapidly with substrate temperature as indicated in Fig. 2.9. This activation behavior exhibits a slope close to that of the vapor pressure of As[9] and strongly suggests that the doping level is due to a thermal source of As in the MBE system. This is quite likely since the system is routinely used for growth of GaAs and associated compounds. Although the system had been partially disassembled, cleaned and baked prior to the Ge growths, it would be very difficult to effectively remove all of the As from such an intricate system, even with extended baking.

An extrapolation of the data presented in Fig. 2.9 indicates that a layer with a carrier density of 1×10^{16} cm^{-3} would result at a substrate temperature of 320°C. However, a growth at this temperature resulted in a p-type layer as shown by the solid datum point in the figure. This reversal in

SC78-683

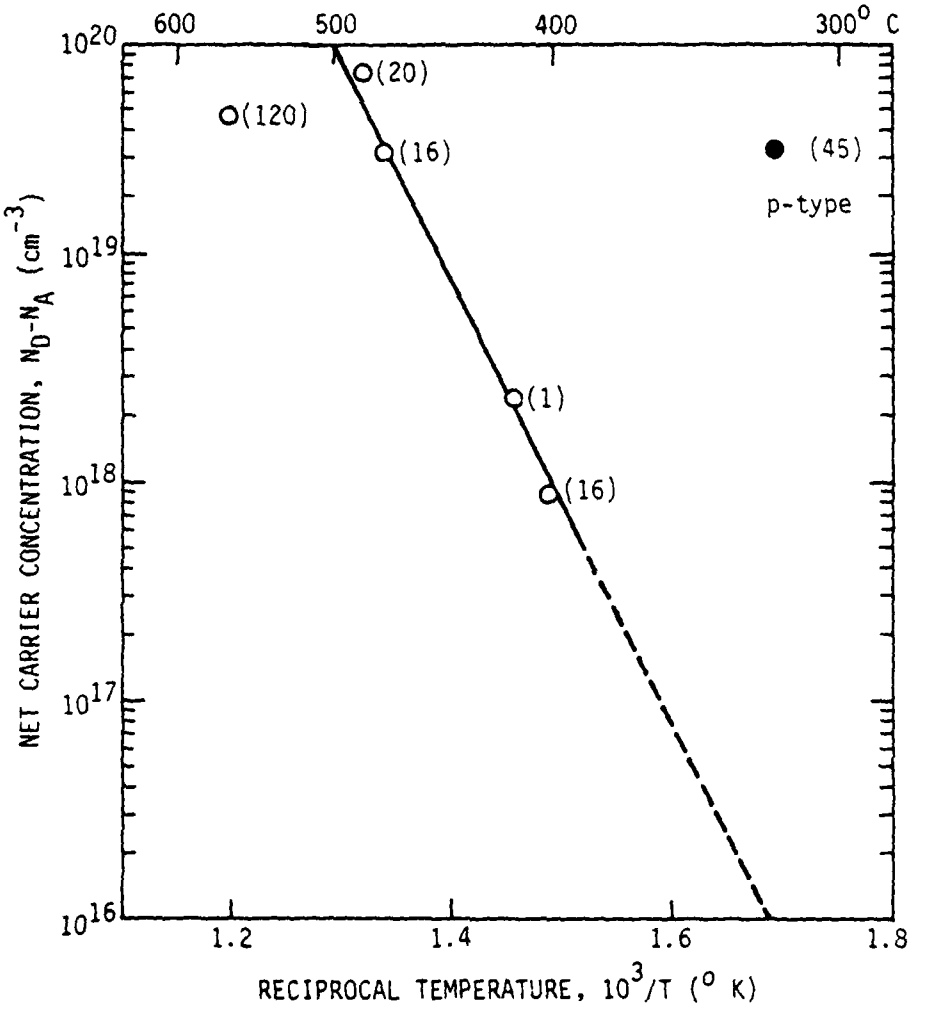

Fig. 2.9 Net carrier density as a function of reciprocal substrate temperature for MBE growths of Ge on GaAs. Numbers in parentheses give growth times for the ~ 1 micron thick layers.

conductivity type may be due to structural defects which are p-type in Ge.[10] Although it may be possible to eliminate such defects by control of growth parameters, it is nevertheless clear that a dedicated system would be desirable to obtain carrier densities below 1×10^{16} cm^{-3}. While one might consider designing a system dedicated to the growth of column IV semiconductors, the desirability of in situ growth of Ge-GaAs heterojunctions would defeat the purpose of having a dedicated system to prevent As poisoning. Thus, based on these results, the MBE investigation was discontinued in favor of another epitaxial technique which combines the favorable aspects of LPE and VPE. The plasma-enhanced CVD technology discussed in the following section is ideally suited for the growth of high purity epitaxial Ge on GaAs as it is not constrained by thermodyanmic considerations, can be initiated with minor relatively inexpensive modifications to an LPE system, and can be made compatible with in situ GaAs epitaxial growth by LPE.

2.3.3 Plasma-Enhanced Chemical Vapor Deposition

Plasma-enhanced CVD is an attractive technique for low temperature deposition of materials that have unfavorable thermodynamic properties or thermal limits of growth by other methods. The thermodynamic limitations imposed on other CVD methods are relieved by the large electron density in high frequency plasmas. Since the electron temperature is typically $>10^4$ K, dissociation of reactant molecules is easily accomplished at low substrate temperatures. Thus, epitaxial growth can then be carried out at temperatures that are adequate for suitable surface atomic mobility.

The next chapter describes in detail the results of the 2-year effort in growing epitaxial Ge on GaAs using the plasma-enhanced CVD technique.

3.0 EPITAXIAL GROWTH USING THE PLASMA-ENHANCED CVD TECHNIQUE

Plasma-enhanced CVD is a very attractive process for growing materials at low temperature and pressure. The plasma, a partially ionized gas composed of ions, electrons and neutral species, is formed through the action of high temperature or strong electric or magnetic field. The various kinds of plasmas are shown in Fig. 3.1. In a r.f. discharge plasma using strong electric field, the free electrons gain energy from the electric field and lose this energy through collisions with neutral molecules, ions and electrons. This kind of glow-discharge is usually characterized by electron energies of about 1 to 10 eV[11] (i.e., electron temperature of ~10^4 K-10^5 K) and electron densities of 10^9 to 10^{12} cm^{-3} in the discharge volume. The energy required to sever existing bonds in molecules is adequately supplied by the hot electron plasma (>10^4 K). Many reactions that are limited thermodynamically are possible with plasma assistance because of this high energy transfer. The products formed from a plasma discharge reaction are all chemically active and thus can form new stable compounds. The sufficiency of the energetic electrons to promote many dissociation and recombination reactions are well demonstrated in the cases of plasma assisted deposition of epitaxial Si, GaN, BN and amorphous Si and Si_3N_4. To describe a plasma fully, the most important parameters that are needed are the electron energies and its distribution. They are discussed in the following section.

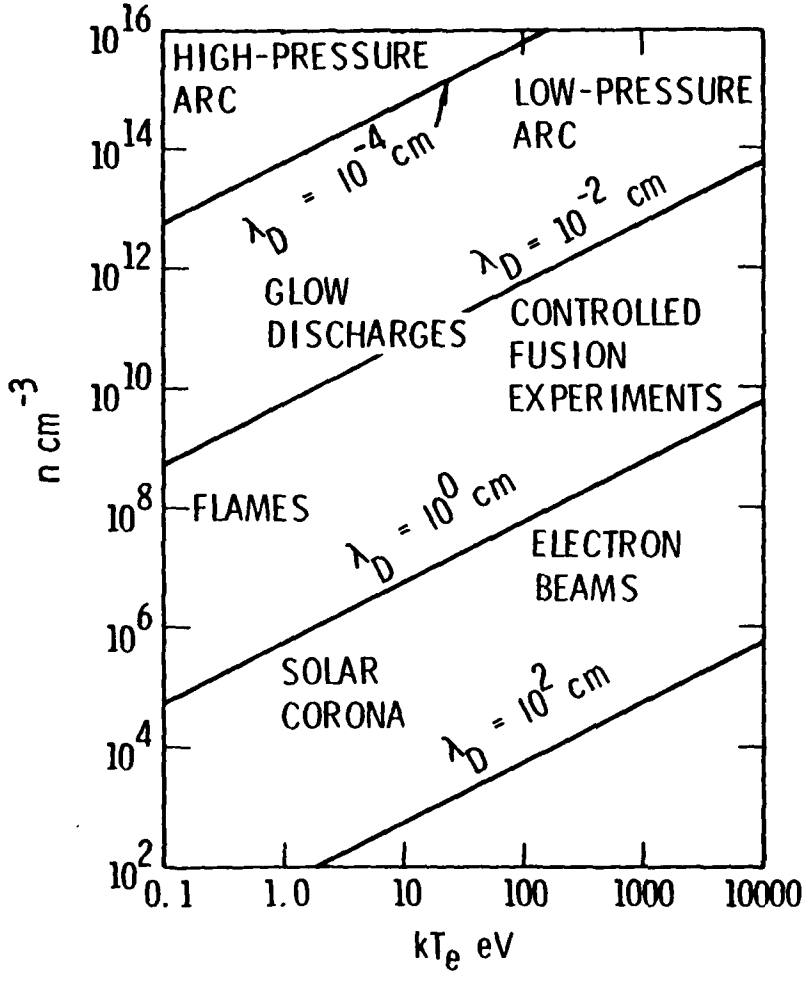

Fig. 3.1 Typical plasmas characterized by their electron energy and density.

3.1 Review of the Plasma-Enhanced CVD

In order to obtain the electron-energy distribution in a plasma, the electron-velocity distribution has to be known. The electron-velocity distribution plays a central role in defining the physical properties of a plasma. From it are derived the electron-energy distribution, the average electron energy, the electron-transport properties and the rate constants for reactions involving electron-molecule collisions. The shape of this distribution is dependent upon the magnitude of the applied electric field and the nature of the elastic and inelastic interactions which the electrons undergo. Elastic interactions are those interactions in which the electrons transfer a small amount of their energies to the kinetic energy of the host molecules, essentially heating up the plasma gas as a whole. Inelastic interactions are those interactions in which the electrons impart a substantial amount of energy to the host molecules to raise them to higher potential energy states, either as metastable species or as ionized species. It is these interactions that promote reactions in a plasma.

By definition, the electron-velocity distribution function $f(\vec{r},\vec{v})$ represents the density of electrons in both position and velocity space. The electron density at the point r is thus

$$n = \int_{-\infty}^{\infty} f(\vec{r},\vec{v})\, d\vec{v}$$

If $\phi(\vec{r},\vec{v})$ defines some property of the electrons which might depend on both position and velocity, the average value of this property weighted against the distribution of velocities can be expressed as:

$$n \langle\phi\rangle = \int_{-\infty}^{\infty} \phi \, f \, d\vec{v}$$

The exact form of the electron-velocity distribution function can be derived through the consideration of the gain and loss of electrons from an incremental volume in phase space defined by dr dv. The equation summarizing the net rate of transfer of electrons from this volume is the familiar Boltzmann equation and is expressed as:

$$\frac{\partial f}{\partial t} + \vec{v} \cdot \nabla_r f + \frac{e\vec{E}}{m} \cdot \nabla_v f = \left(\frac{\partial f}{\partial t}\right)_{coll}$$

By expressing the distribution function f as the sum of an isotropic distribution f° and an anisotropic distribution $\phi(\vec{v})$; and by further assuming that this anisotropic contribution is largest when $\vec{v}$ is in the direction of the gradient or force causing the perturbation and smallest when it is perpendicular to it, f can be written as:

$$f = f^\circ + \phi(\vec{v}) = f^\circ + \frac{\vec{v}}{v} \cdot f'$$

Substituting this f into the Boltzman equation gives two equations involving f° and f', the values of which can be solved for specific collision processes.

In general, it is difficult to characterize any plasma completely because not all the physical parameters affecting it are well known. All the collision processes as well as the various ionization levels and potentials will affect the nature of the plasma itself. However, in the particular case of a dilute amount of a certain molecule in a well characterized host gas, it is conceivable that the dilution causes only small perturbation in the host gas and that the behavior of the plasma can be reasonably approximated by that of the host gas. In the specific case of a 1% GeH_4 in H_2, it is felt that the perturbation due to the 1% GeH_4 is small and therefore the plasma dissociation of GeH_4 in H_2 can be understood through a study of the H_2 plasma. Dreicer[12] has calculated numerically the electron-velocity distribution for a hydrogen plasma, taking into account inelastic collisions as well as random two-body coulombic collisions. Elastic collisions between electrons and hydrogen molecules are neglected on the basis that they represent only a small energy loss term. In consideration of the coulombic interactions only those occurring between two electrons are retained since it is shown that electron-ion encounters result in negligible energy losses from the electron.

Figure 3.2 illustrate the numerical solutions obtained for E/p equal to 28.3 V/cm-torr, which is the electric field-pressure ratio required for breakdown of the hydrogen plasma. The function plotted on the ordinate is the electron-energy distribution function which $f(\varepsilon)$ is related to the velocity distribution function $f^\circ(v)$ by:

$$f(\varepsilon) = \frac{4\pi}{m} v f^\circ(v)$$

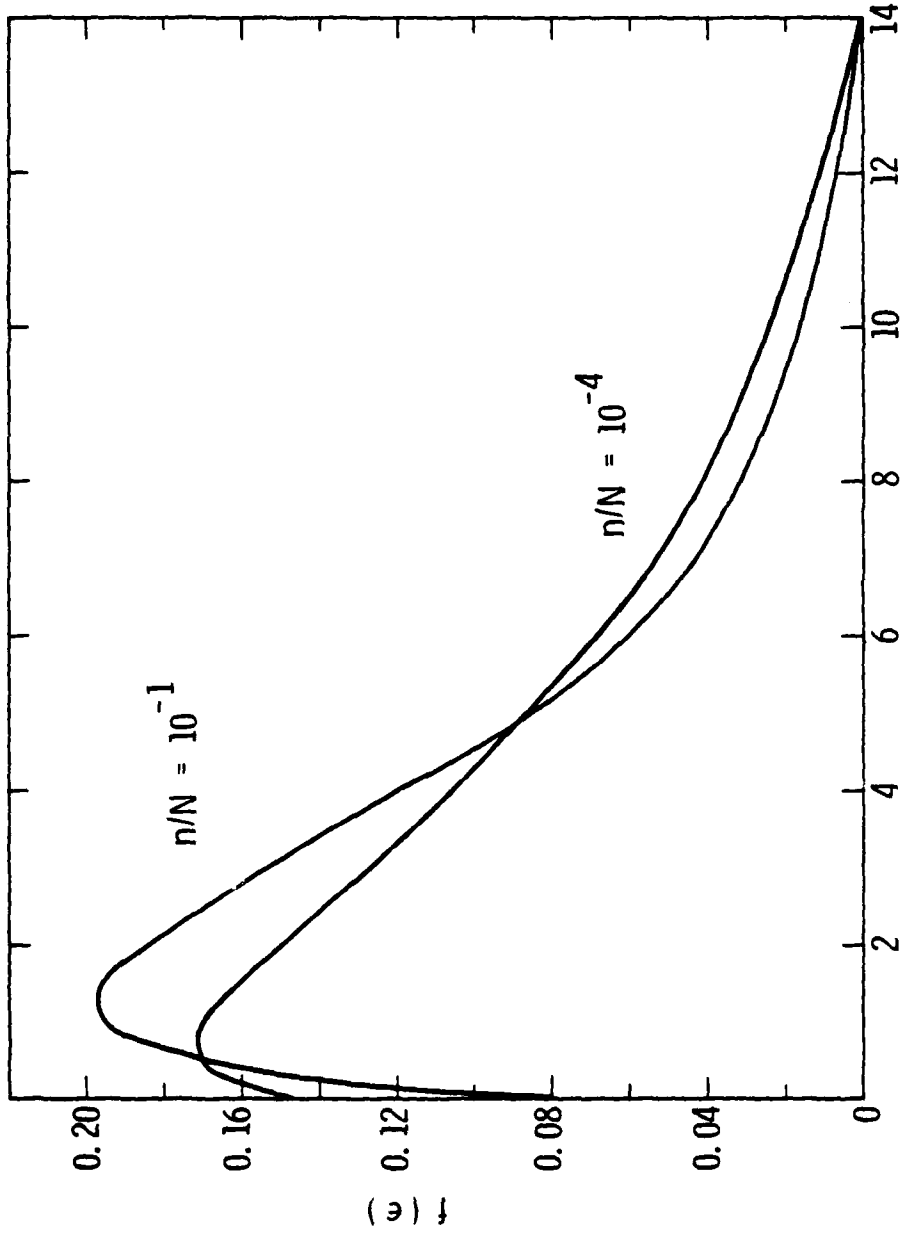

Fig. 3.2 Effect of the extent of ionization (n/N) on the energy distribution function for a hydrogen plasma.

where $\varepsilon = 1/2\ mv^2$. For each value of electric field-pressure ratio, E/p, the effects of the extent of ionization are identified by the value of n/N. At very low energies, the electron-energy distribution function $f(\varepsilon)$ decreases as the extent of ionization increases. In the neighborhood of 1 eV, the distribution cross each other and the situation is reversed. At still higher energies, the distribution cross each other two more times until in the very high-energy tail, the population increases with the degree of ionization. At the highest degree of ionization the distribution function is very nearly Maxwellian.

The effects of electron interactions on the average energy $\langle\varepsilon\rangle$ are illustrated in Fig. 3.3. As the degree of ionization increases, the average energy first rises and then falls. The rise is attributed to the fact that the slow electrons produced in inelastic encounters exchange energy with other electrons, and are quickly redistributed over the body of the distribution. The subsequent fall in average energy as n/N increases even further reflects the fact that coulomb encounters have decreased the population in the neighborhood of the first excitation potential and have redistributed these electrons primarily into lower energy regions. Ultimately, when n/N becomes large enough so that the rate at which electrons exchange energy with each other greatly exceeds the rate at which they gain energy from the field, the distribution function becomes Maxwellian. For any n/N, increasing E/p also increases the average electron energy $\langle\varepsilon\rangle$. With E/p = 28.3 V/cm-torr as shown in Fig. 3.3, the corresponding electron energy $\langle\varepsilon\rangle$ is approximately 3.7 eV for values of n/N ranging from 10^{-1} to 10^{-5}. For E/p = 49.8 V/cm-torr, $\langle\varepsilon\rangle \approx 4.7$

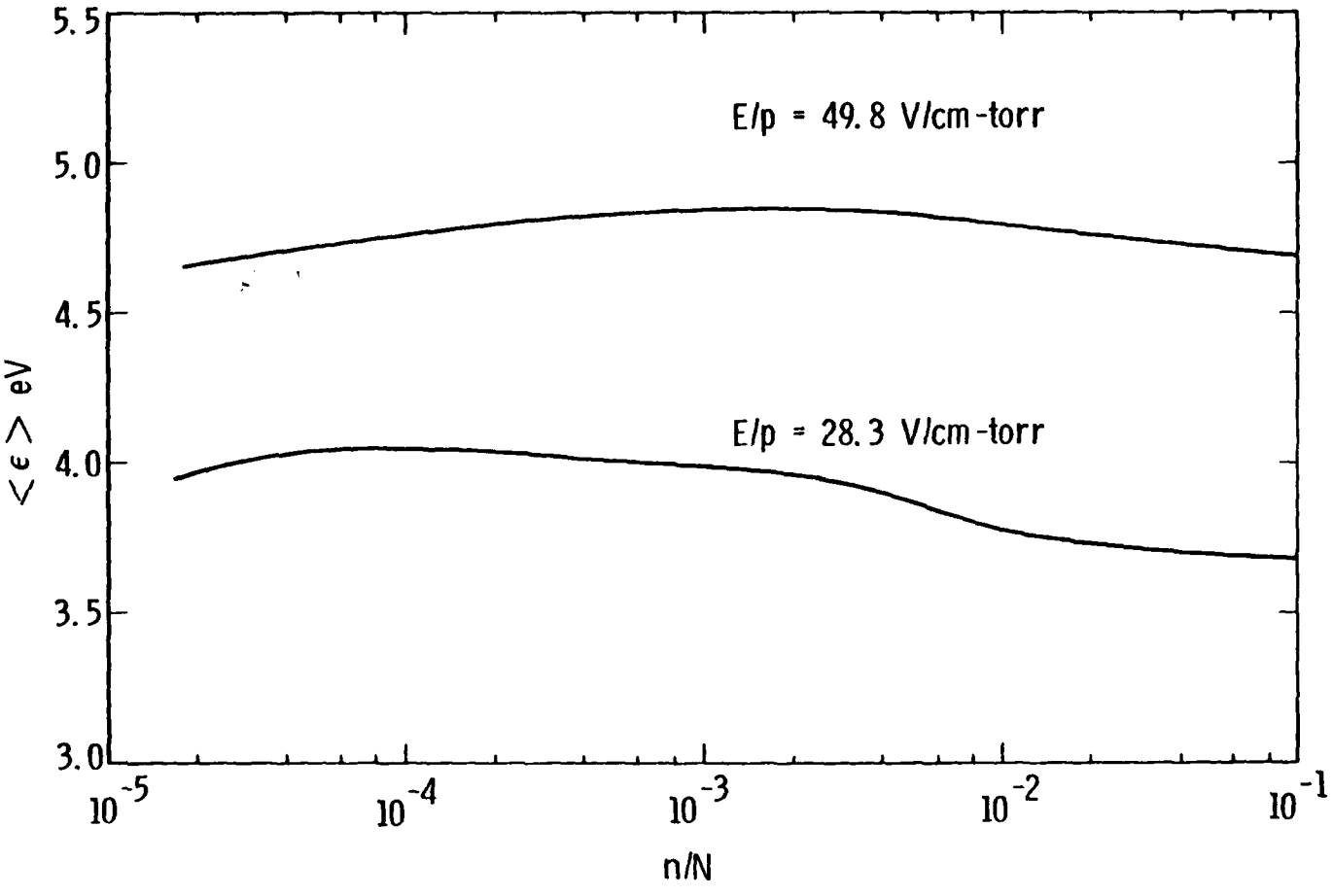

Fig. 3.3 Effect of ionization n/N on the average energy <ε> at different E/p values.

eV. Even though $\langle\varepsilon\rangle$ is only a few eV, a significant amount of electrons can still be found with higher energies because of the distribution as shown in Fig. 3.2. With a H_2 plasma, GeH_4 can easily be ionized by colliding with the excited electrons or hydrogen since the ionization energy of GeH_4 is ~12.3 eV.[13] The appearance potential $A(Ge^{+\cdot})$ of the following reaction:

$$GeH_4 + e \rightarrow Ge^{+\cdot} + 2H_2 + 2e$$

which results in the formation of the $Ge^{+\cdot}$ ion is 10.7 eV.[14] The strength of the Ge-H bond in GeH_4 is ~3 eV.[14] Other excited species, e.g., GeH_3^+, GeH_2^+, and GeH^+ have ionization energies of ~12-14 eV.[13]

Our experimental results indicated that Ge can indeed be grown from a mixture of GeH_4 and H_2 only with the assistance of a plasma. Pyrolysis of GeH_4 at a temperature that is even higher than that routinely used for plasma growth gave negligible deposition of Ge.

3.2 PECVD Growth System

Three major modifications have to be performed on a conventional LPE system before it can be used for the PECVD experiment. They are:

1. Addition of a pressure controlling system capable of maintaining a low presure,
2. Introduction of rf voltage, and
3. Input gas manifold.

The furnace that was used was a transparent furnace previously used in the LPE growth of Ge on GaAs. Transparent furnaces are widely used in the LPE growth of semiconducting materials, especially in the ternary and quaternary compound areas because of their ease in allowing the visual determination of the exact melt saturation temperature. A transparent furnace is used in the PECVD growth of Ge because it is necessary to observe and control accordingly the spatial distribution of the plasma. The transparent furnace is heated with a resistive element. A graphite susceptor with two wire-wound heating elements embedded in it was also constructed. This provides an independent source of heating the substrate alone. Cold wall, as well as hot wall growth experiments can be performed.

In the conventional LPE growth system, the exhaust gas simply vents out to the atmosphere through a bubbler. However, in the PECVD growth system, such a venting process is not feasible because the growth chamber is operating under a low pressure. Thus a suitable output gas handling manifold capable of maintaining a clean, oil-free, low pressure growth chamber as well as providing a controlled exhaust for the gases is needed. This is achieved through the use of cryogenic pumps. They provide fast, clean pumping of the chamber and by throttling the valves, they can be used to control the chamber

pressure independent of the flow-rate of the input gas. For rf coupling, a low power, 13.5 MHz rf source is capacitively coupled to the graphite susceptor. The graphite susceptor acts as the grounded terminal of the rf voltage. The other terminal, or the hot terminal, is a mesh screen located outside the quartz furnace tube. Later on in the program when doping experiment was anticipated and performed, the graphite susceptor was replaced by a stainless steel susceptor covered by a quartz plate. The degree of purity achieved by the two susceptors are essentially the same. The stainless steel susceptor is superior to the graphite boat in that it minimizes the memory effect associated with absorbed dopant gases by the graphite susceptor.

At the beginning of the PECVD-Ge program, a simple but effective gas manifold was constructed with mass flow controllers which allowed controlled amount of GeH_4 mixture, H_2 and etchant gases to be fed into the growth chamber independent of each other. This manifold, however, was found indequate in handling the controlled multiple-doping experiments that was performed later. Consequently, a new manifold was designed and constructed. This is shown schematically in Fig. 3.4. The three 1-litre gas storage cylinders can be pre-mixed to the desired doping levels prior to growth. During growth, the input flow of the various gases are controlled by mass flow controllers while the chamber pressure is maintained by the cryogenic pumps to ~ 2 to 10 torr, with the higher pressure most often used for stabilizing the plasma as well as minimizing sputtering effects. By turning the storage cylinders on and off during the course of the growth, multi-layer structures can be obtained.

ERC80-9234

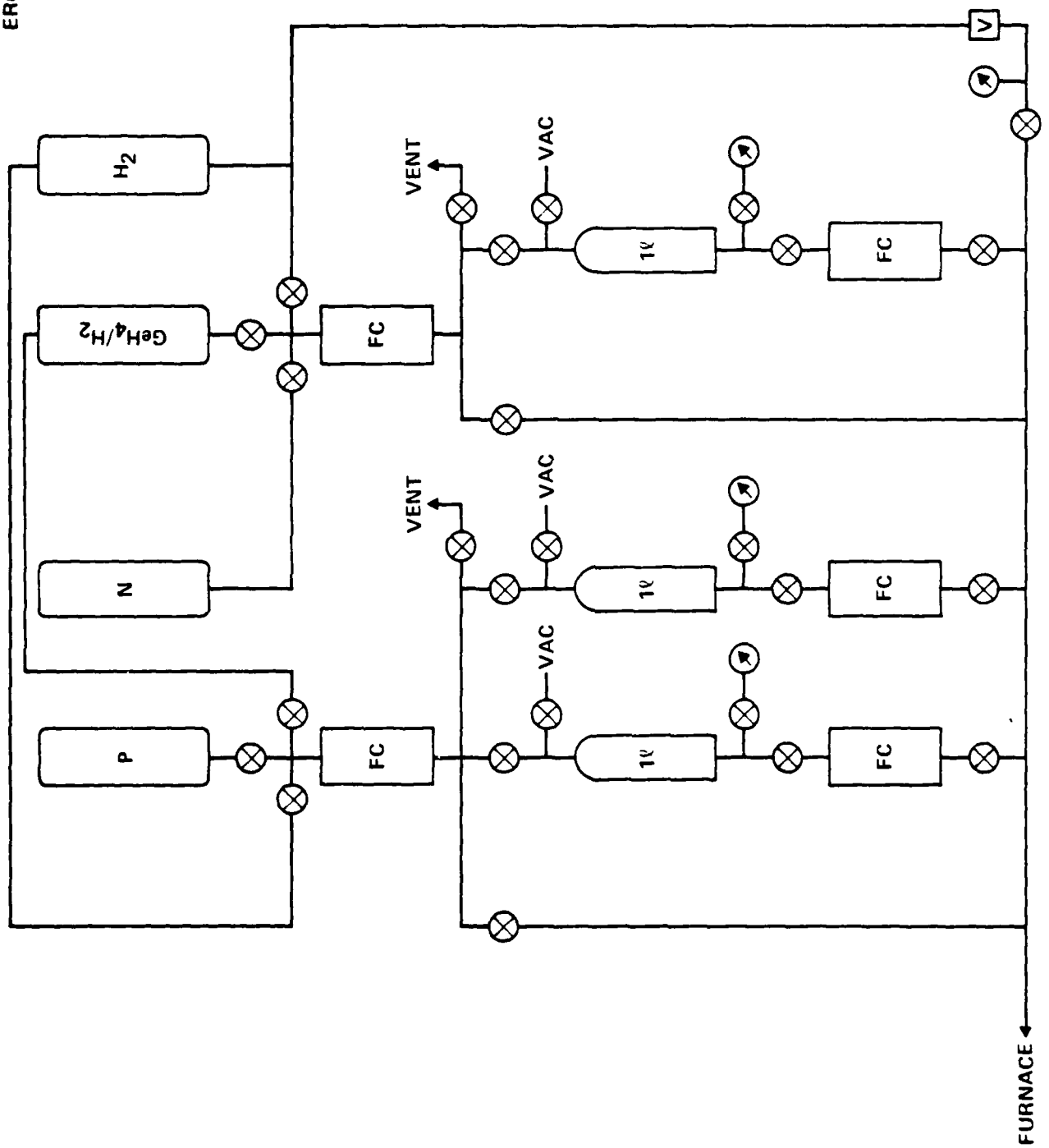

Fig. 3.4 Schematic diagram of the plasma-enhanced CVD apparatus.

3.2.1 Growth of Ge on GaAs Using PECVD

A typical growth cycle is shown in Fig. 3.5. The bottom curve is a plot of the growth chamber pressure as a function of time, while the top curve is the substrate temperature as a function of time. Various etching schemes were tried before loading the GaAs substrate into the chamber. A 5 min etch in warm 5:1:1::H_2SO_4:H_2O:H_2O_2 followed by a 5 min soak in concentrated HCl gave satisfactory results. After etching, the GaAs substrate is loaded into the chamber which is then pumped down to a low pressure. Hydrogen is introduced into the chamber as it is heated to ~600°C. This serves as a final clean-up of the GaAs substrate before growth. The substrate was never heated to a temperature higher than 635°C which is the limiting temperature at which Ga and As evaporate congruently from GaAs.[15,16] This bake-out temperature is also above the well-established temperature of 525-535°C[17] at which the passivating oxide film on GaAs evaporates. After the high temperature bake-out, the system is cooled to the growth temperature of around 425°C to 450°C. This growth temperature permits epitaxial growth without plastically deforming the Ge.[18] Controlled flow of the reactant gases is then introduced, the r.f. power is turned on and growth proceeds. After a certain growth time, the system is turned off and growth is terminated. Because the growth of Ge is solely accomplished by the plasma dissociation of GeH_4, and since very little Ge is formed from the pyrolysis of GeH_4 at ~450°C, very abrupt termination can be obtained. This growth characteristic is a major advantage in the growth of abrupt p-n junctions by Plasma Epitaxy.

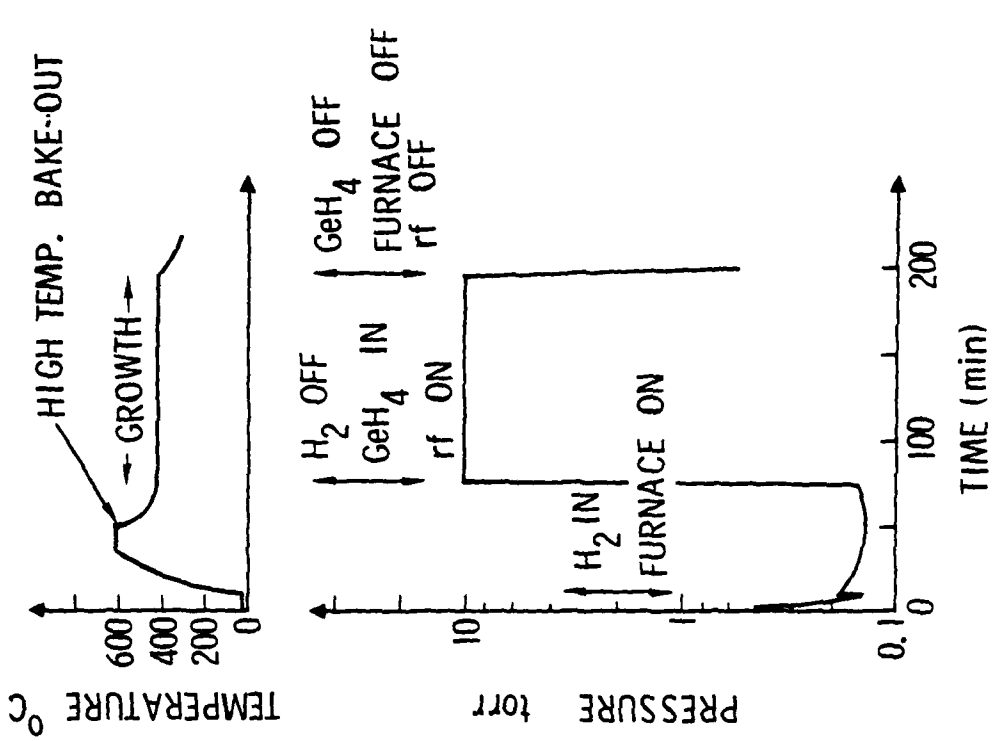

Fig. 3.5 Temperature and pressure of a growth cycle.

Later on in the program, when it was apparent from the results that there was a "pile-up" of carrier near the Ge-GaAs interface, various caustic and acidic etchants were tried to determine if this "pile-up" was caused by the etchant. No correlation of any kind was found.

Plasma etching of the substrate before growth was also investigated. CF_4 plasma and H_2 plasma were used. Details of the results will be discussed in the next section.

3.3 Results and Discussions

In the study of the growth of Ge using plasma-enhanced CVD, the properties of the grown Ge are good indicators of the success and feasibility of the technology.[19,20] Crystal properties such as purity, crystallinity, surface morphology and doping capability are studied. It is found that the purity of the Ge layers is extremely good exhibiting theoretical drift mobility at the 10^{16} cm^{-3} level. Smooth, single crystalline Ge are also routinely obtained for growth temperatures greater than 425°C. Doping experiments using the plasma dissociation of B_2H_6 were performed and p-type layers were obtained. *In situ* growth of Ge p-n junctions were also possible with PECVD. The following sections describe these results in greater detail.

3.3.1 Purity

In the earlier attempts of growing Ge on GaAs using LPE, layers with carrier densities $>10^{18}$ cm^{-3} were obtained. These higher carrier densities

were probably due to thermodynamic instabilities at the melt-seed interface, resulting in dissolution of a few monolayers of GaAs and subsequent autodoping of the Ge single crystal. In the present system using PECVD, a different kind of growth mechanism exists. The plasma growth is essentially nonequilibrium in nature, and the purity of the grown layers is determined primarily by the purity of the reactant gases and the materials used. Since epitaxial layer purity is a special concern in this system, the reactant GeH_4 has been selected on the basis of its high purity and availability. Epitaxial Ge layers with carrier densities as low as 10^{14} cm^{-3} have been obtained from GeH_4 pyrolysis on Ge substrate. This ultra high purity (UHP) GeH_4 as well as UHP H_2 were used in the PECVD of Ge.

A meaningful way to determine the purity of a grown layer is to measure its carrier concentration and mobility and compare them to the theoretical values. Figure 3.6 is a plot of the mobility of the carriers as a function of the free carrier concentration at room temperature. The solid lines are the theoretical electron and hole drift mobilities of uniformly doped bulk Ge. The data points are drift mobilities which are obtained from appropriately adjusting the measured Van der Pauw mobilities by the Hall factors. Various reactant gases as well as different boats were used as shown in the figure. There are several important points to be discussed here:

1. The p-type layers that are grown from a GeH_4/H_2 mixture have very good mobilities, approaching those obtained from bulk Ge

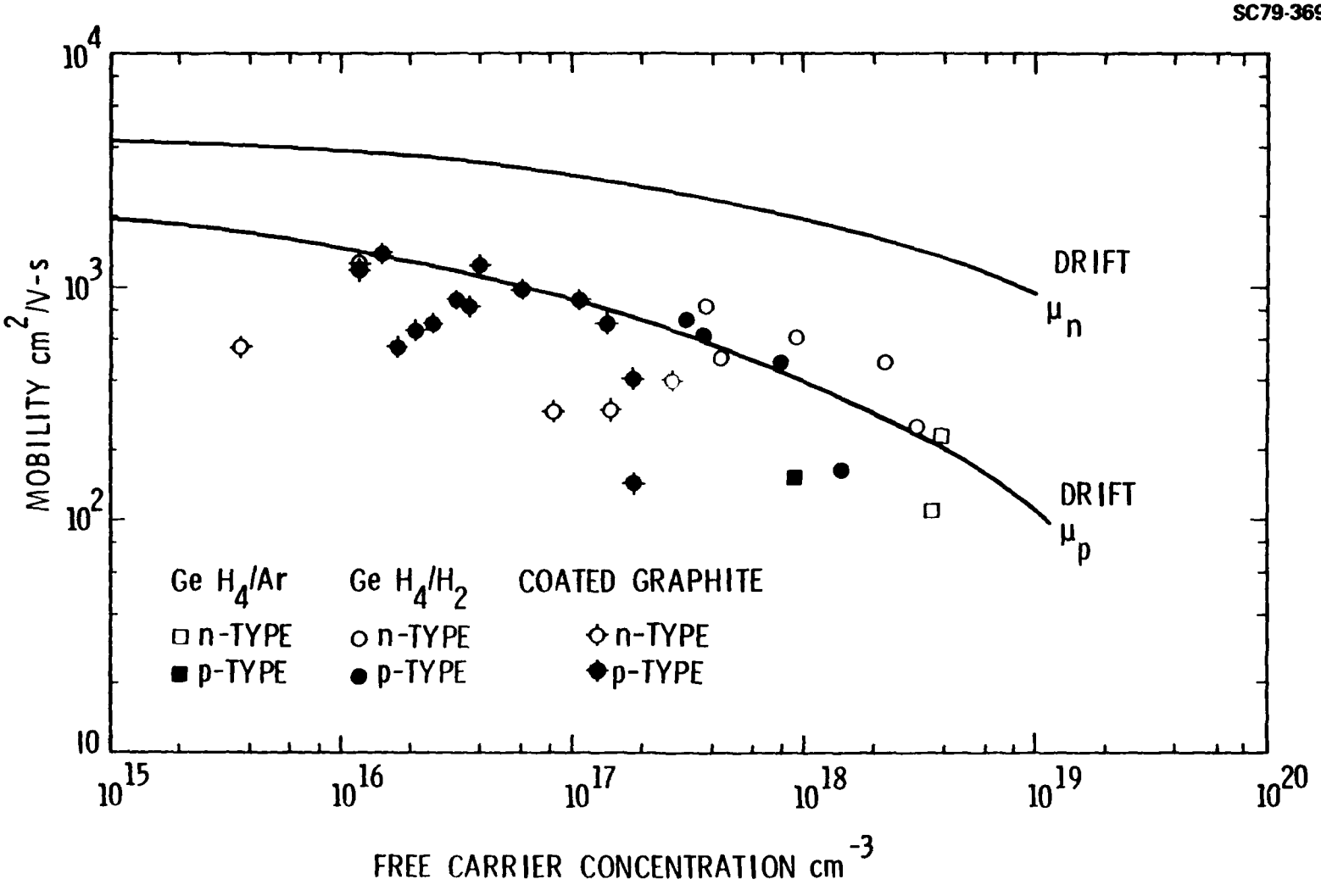

Fig. 3.6 Carrier concentration and mobility results of Ge layers grown by PECVD.

crystals. The lowest carrier concentration obtained is $<10^{16}$ cm^{-3}.

2. All the n-type layers are compensated; the highest mobility obtained is around 1000 $cm^2/V\text{-}S$. For a non-uniformly doped layer, n and μ are functions of the thickness of the layer. If a certain thickness of a layer is compensated, then even though the rest of the layer have theoretical mobility, the whole layer would still appear to be compensated on this average n vs average μ plot. Therefore in order to fully understand this, the n (x) and μ (x) as a function of the thickness of the layer are investigated. They are reported later in the differential Van der Pauw result.

3. When a pyrolytically coated UHP graphite susceptor was used instead of an uncoated one, a reduction of over an order of magnitude in the free carrier concentrations of the layers was obtained. Mobilities too were improved. However, no discernible difference was observed when a stainless steel boat with a quartz covering plate was used instead of the pyrolytically coated graphite boat.

4. Ge layers grown from GeH_4/Ar mixture do not have good electrical characteristics. They have low carrier mobilities and are quite compensated.

If the average carrier concentration of a layer is plotted against the thickness of the layer, curves as shown in Fig. 3.7 can be obtained. In Fig. 3.7, each different symbol represents a different layer preparation. Again, several observations can be made.

1. For a certain layer thickness, the average n of a layer is not dependent on the way the layer is prepared.

2. For layers <0.5 μm thick, there is a gradual increase in the carrier concentration as the layer becomes thinner, eventually becoming $>10^{19}$ cm^{-3} for thin layers < 800 Å thick.

3. For thick layers, the average n appears to reach an asympotic value. Together with 2 above, it indicated that the layers have a high carrier concentration near the interface, but eventually levelled off to the background carrier concentration.

4. Using pure GeH_4, the average carrier concentration for layers thicker than ~ 0.5 μm is ~ 2×10^{18} cm^{-3}. This can be due to the purity of the starting GeH_4 gas.

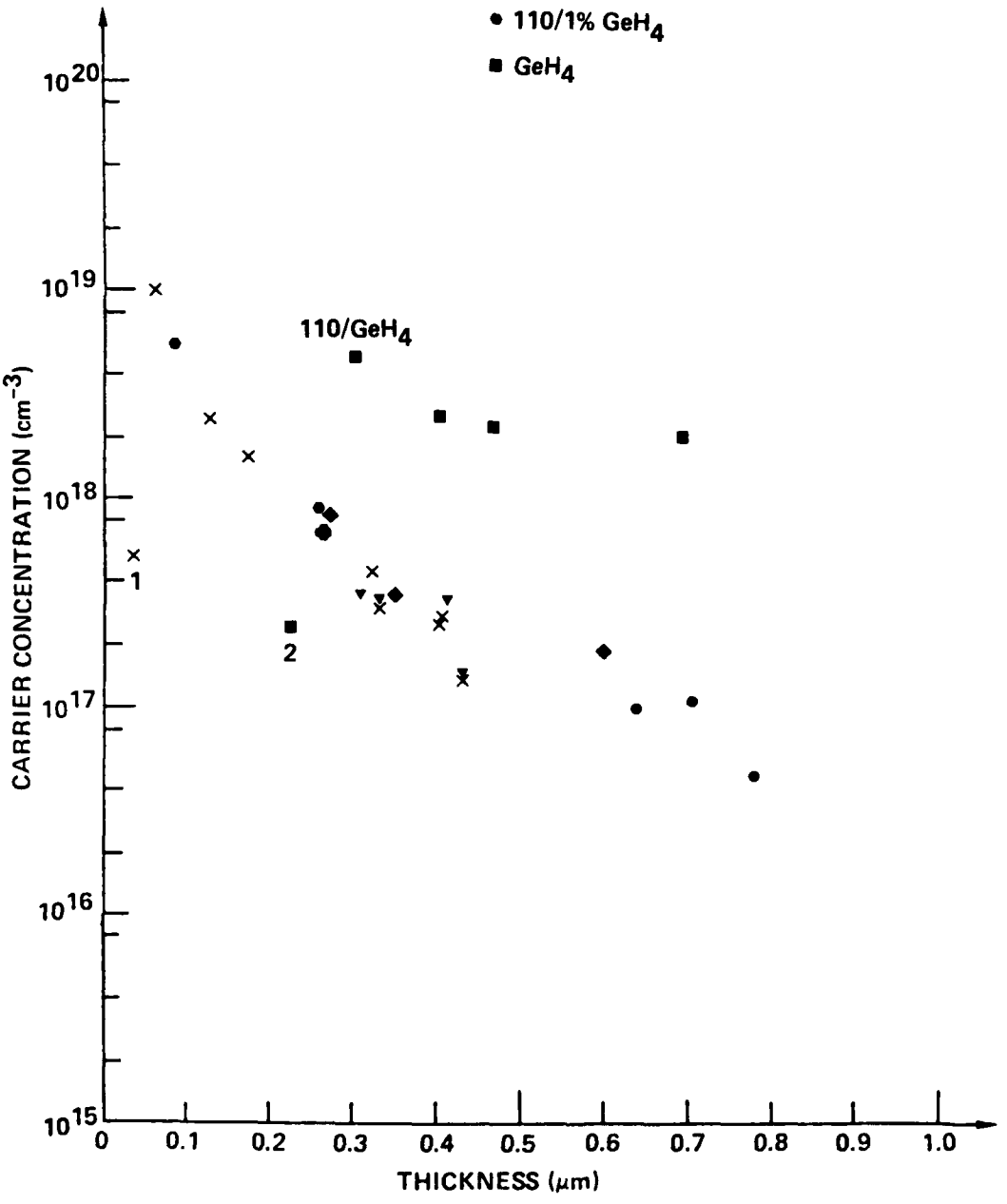

Fig. 3.7 <n> vs thickness of layers grown using PECVD.

5. No improvement in the purity of the layer is seen when growth is performed in a used (Ge deposited) liner. The x's are consecutive layers that are grown from the same liner. The general behavior of the purity of these layers are similar to all the other layers.

6. No improvement is seen in the purity of layers grown on (110) or (111) oriented GaAs. However, the surface morphology is different for each type.

7. The particularly low carrier concentration in isolated cases (e.g., datum points marked 1 and 2) are due to heavy compensations in the layers as shown by their low mobilities.

Another way of determining the purity of the Ge layers is to investigate the mobility and carrier concentration as the crystal is grown. This can be obtained from a plot of the differential Van der Pauw results as a function of depth. This technique involves measuring the sheet resistivity and the sheet Hall coefficient of a layer, then etching a measured amount of the layer away and measuring the sheet resistivity and the sheet Hall coefficient of the remaining layer. This is repeated until the entire layer has been etched off. If the layer is wholly n-type or p-type, the sheet resistivity and sheet Hall coefficients before and after etching may be used to calculate the carrier concentration and the carrier mobility of the material that was

removed. Figure 3.8 illustrates this point for a p-type layer. The upper curve shows the carrier concentrations as a function of depth of the layer. The Ge-GaAs interface is located at ~ 1.6 μm, the layer has a fairly uniform doping concentration of ~ 3×10^{16} cm^3 and hole mobility around 1500 cm^2/V-s. This is the background characteristics for this growth cycle. For growth near the interface, i.e., growth less than ~ 0.6 μm, there is a definite increase in the carrier concentration as well as a drop in mobility. Figure 3.9 shows the n (x) for two different layers. Significant dissociation of impurities from the walls of the growth chamber and the substrates and their subsequent incorporation at the onset of the plasma, as well as measurement errors, can account for this carrier "pile-up" near the interface. Note the good reproducibility of these two runs.

3.3.2 Crystallinity

By nature of the low temperature, microscopically hot plasma, metastable reaction species are available for the deposition of Ge. This circumvents the normal thermodynamic limitations of thermal decomposition. In this manner, the deposition temperature could be optimized around the crystal perfection of the epitaxial layer sought. An optimization of surface mobility with electrical properties, is desired. It has been demonstrated that Ge and Si deposited with plasma assistance at 300°C are amorphous in nature but at growth temperature of 700-800°C Si[21] becomes single crystalline. In the PECVD of Ge on GaAs we have found that a growth temperature of >425° is necessary to give a single crystalline Ge layer.

SC79-3715

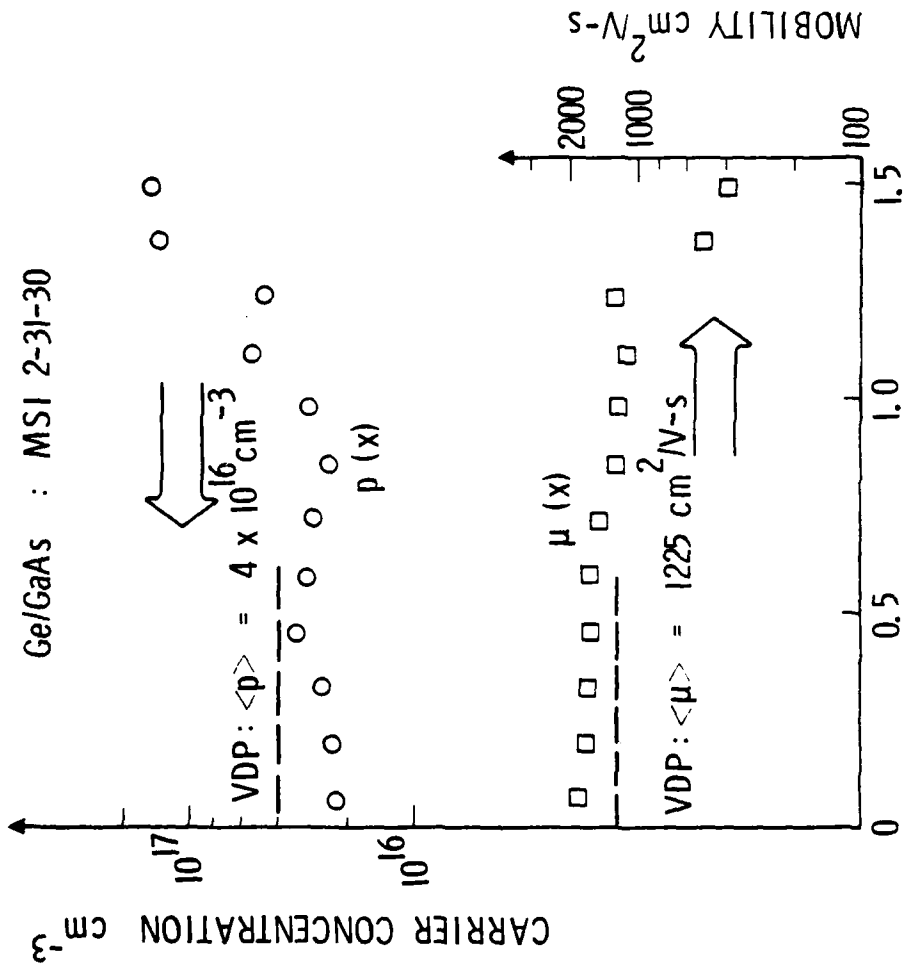

Fig. 3.8 Differential van der Pauw results showing carrier concentration and mobility as a function of thickness.

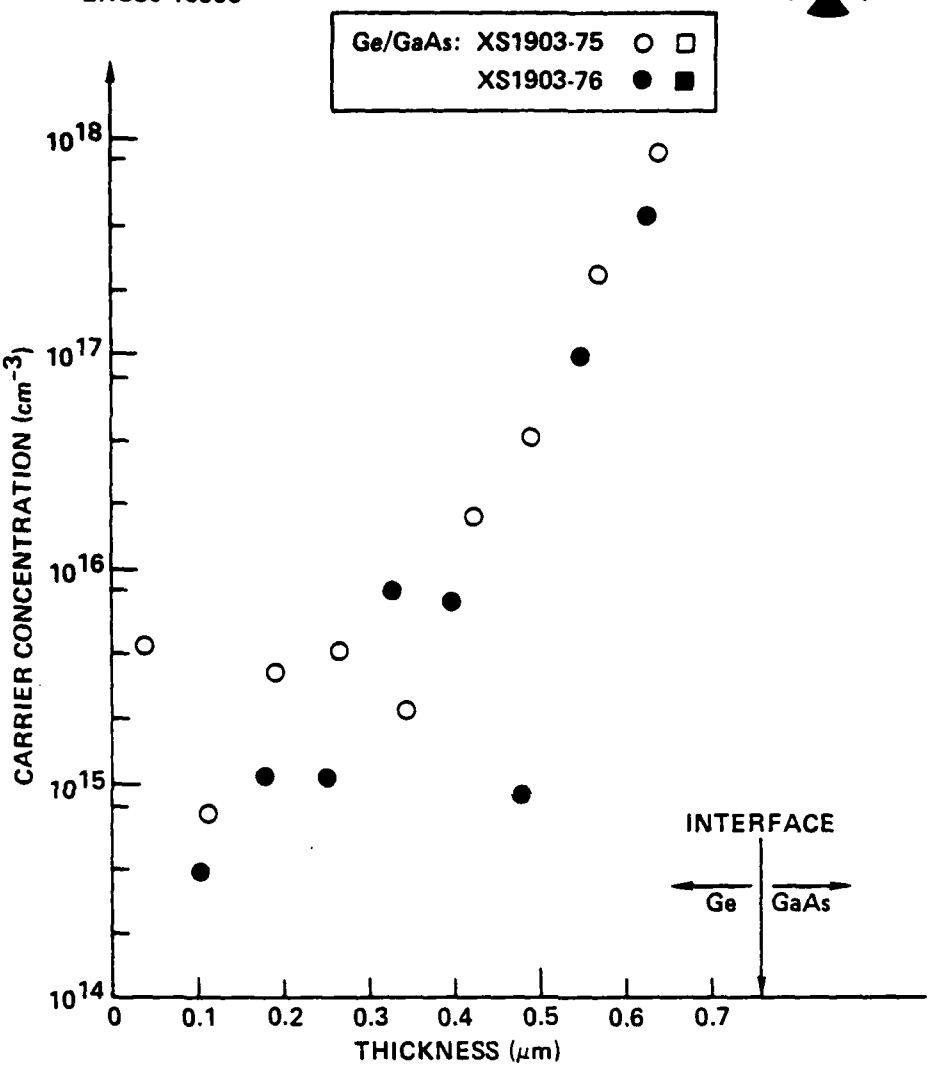

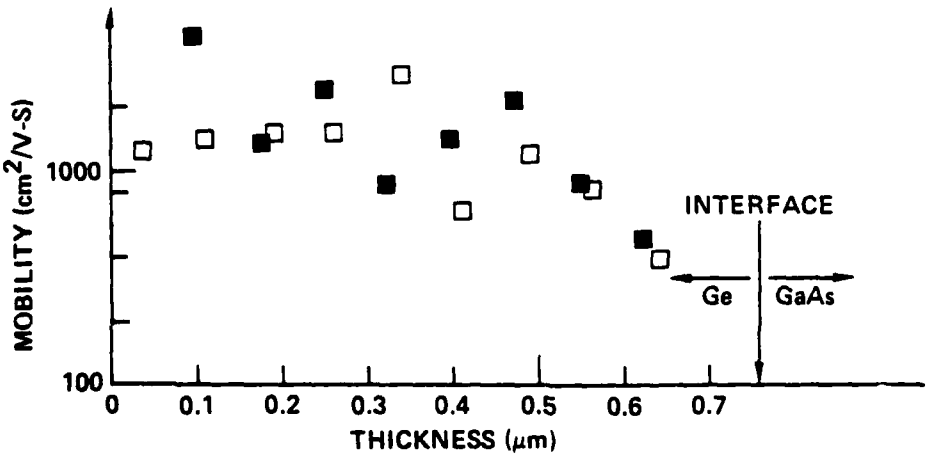

Fig. 3.9 Differential VDP results for n-type layers.

Figure 3.10 is a TEM picture of a Ge layer grown on GaAs at 400°C. A low energy ion beam, sputtering at a low specimen temperature, is used to reveal the Ge layer from the GaAs substrate side. This TEM picture, which shows the crystallinity of the Ge close to the Ge-GaAs interface, shows that the Ge is amorphous. However, when a thicker region of the Ge layer is analyzed by TEM, well defined spots as well as Kikuchi lines are observed, as shown in Fig. 3.11. This indicates that amorphous Ge is obtained near the interface, but it quickly becomes crystalline as it grows thicker. This is understood by assuming that at 400°C, the Ge that first arrived at the GaAs substrate does not have enough energy to move around for a proper lattice site on the GaAs. The amount of energy that it needs depends on the way the GaAs surface is prepared. Once a thin layer of Ge is deposited on the GaAs, Ge that subsequently arrived will be deposited on Ge and at 400°C, the deposition is epitaxial. This observation is analogous to the deposition of Ge on GaAs by evaporation and MBE. It has been observed that Ge deposited on GaAs by evaporation is epitaxial when the substrate temperature is above 350°C,[22] whereas it is also shown that Ge can be grown epitaxially on Ge even at room temperature.[23]

At growth temperature of 426°C, crystalline Ge is obtained on GaAs as shown by the TEM picture in Fig. 3.12.

3.3.3 Morphology and Metallurgical Interface

For device applications, it is essential that the Ge layers be mirror smooth, continuous and have a sharp interface. Using plasma deposition, it is

SC79-6386

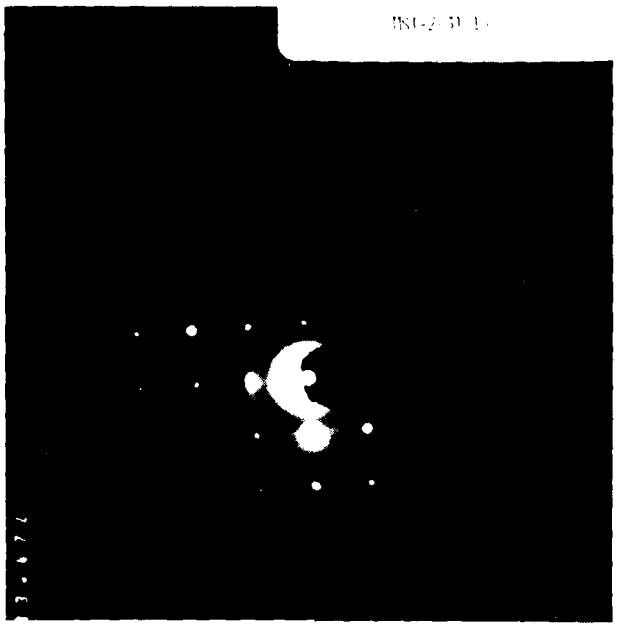

Fig. 3.10 Transmission electron diffraction pattern of a layer grown at 400° C.

SC79-6384

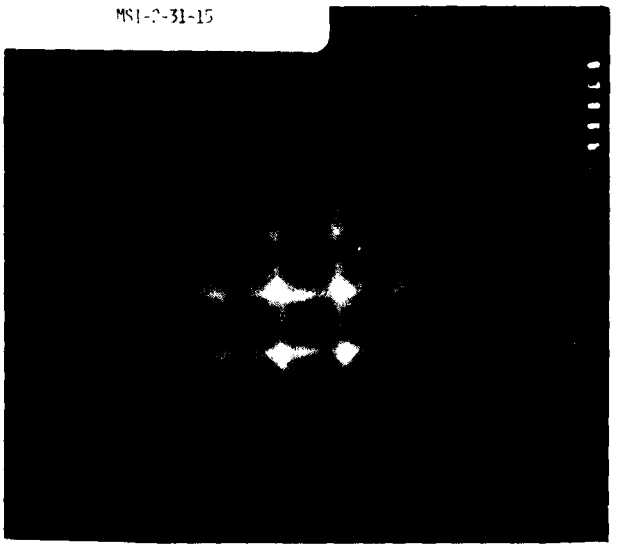

Fig. 3.11 Kikuchi lines observed in Ge grown at 400° C.

SC79-6385

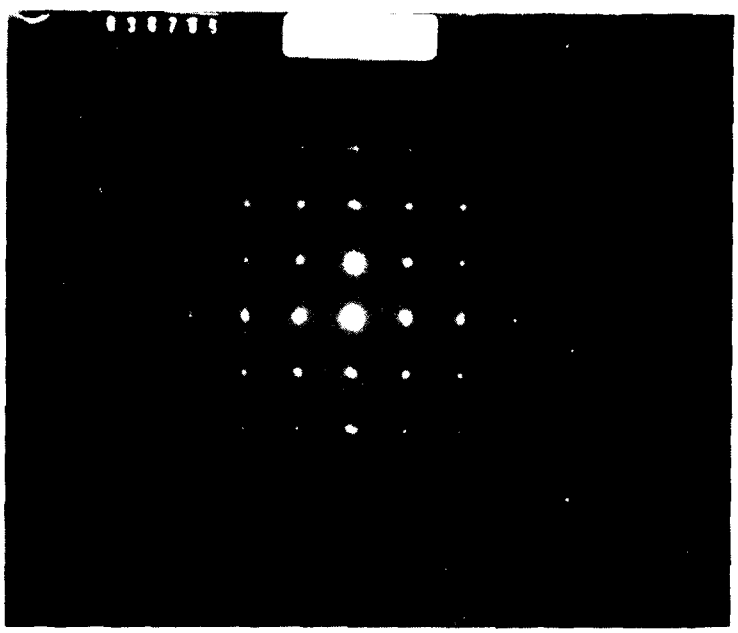

Fig. 3.12 Transmission electron diffraction pattern of a layer grown at 426°C.

possible to obtain layers that have the above qualities. Si_3N_4 deposited by plasma techniques have shown extremely uniform properties with virtually no pinholes (SiH_4, NH_3). Uniformity in the range of ±2.5% has been reported. Since the growth of Ge in our case is epitaxial in nature, it is even more important to control the growth so the best surface morphology is obtained.

Our results show that the morphology of the Ge layers are intimately related to the growth rate of the Ge. At low Ge growth rate, <0.3 μm/hr, rather smooth, continuous layers that have a sandy texture are obtained as shown in Fig. 3.13. At high growth rate, > 0.8 μm/hr, layers with pinholes are obtained as shown in Fig. 3.14. By properly adjusting the input flow-rate and the deposition rate, it is possible to obtain device quality layers as shown in Fig. 3.15. When examined using a Dektak, the surfaces of these layers show a peak to peak variation of 50Å high with a period of about 20 μm as shown in Fig. 3.16. The surface morphology is dependent on the orientations of the substrates. From the PECVD results, it appeared that (110) gave the best surface morphology, followed by (111)B and finally the (100) orientation. For layers that exhibit pinholes there is a linear relationship between the size of the pinholes and the thickness of the layer as shown in Fig. 3.17. Although there is considerable scattering, extrapolation to a zero pinhole size shows that the pinholes originate at the Ge-GaAs interface. The large pinhole size even for a thin layer and the high density of them can be very objectional to device applications.

The profiles of Ga, As and Ge through the heterojunction interface has been studied using Secondary Ion Mass Spectroscopy (SIMS). Very abrupt

SC79-6389

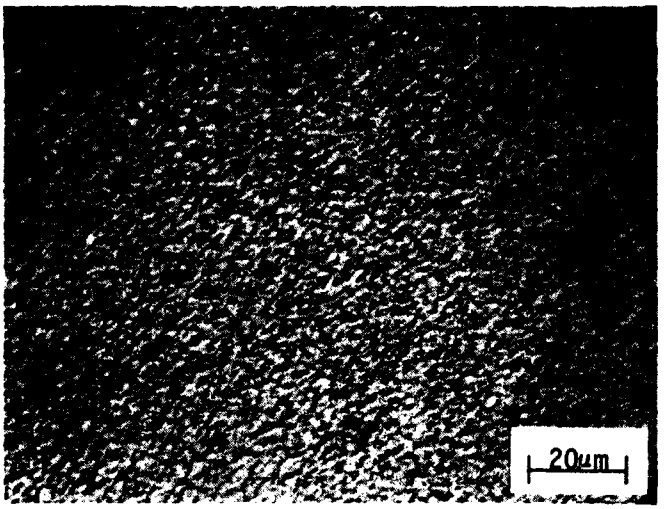

Fig. 3.13 Surface morphology of a layer grown with a low growth rate.

SC79-6388

Fig. 3.14 Surface morphology of a layer grown with a fast growth rate.

SC79-4419

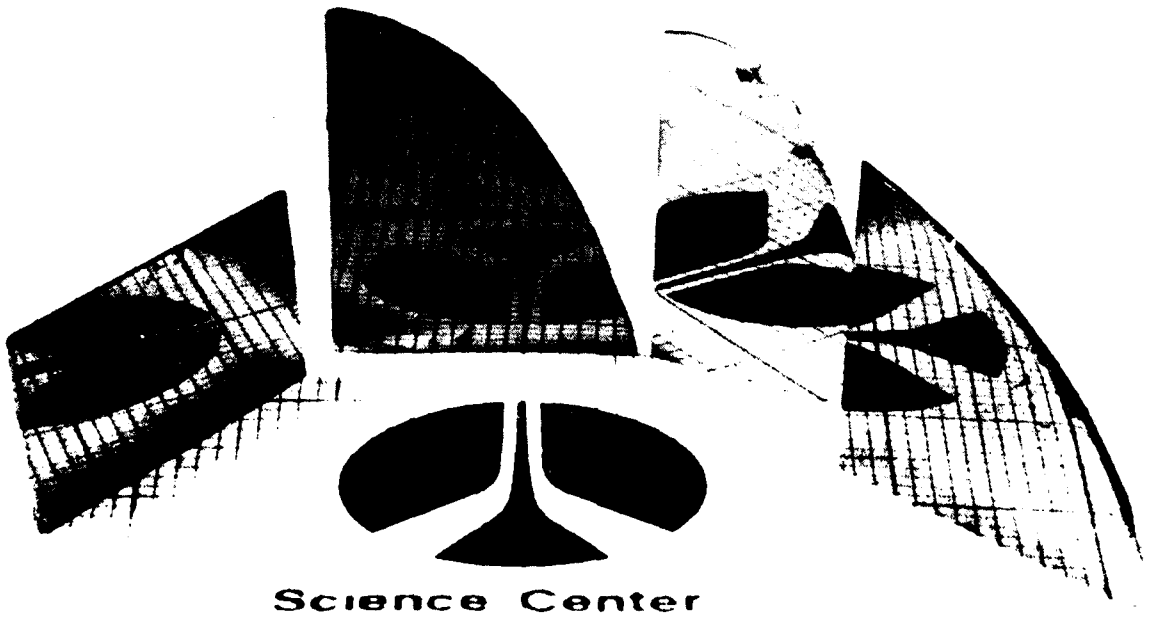

Fig. 3.15 Mirror smooth epitaxial Ge layers grown on GaAs using PECVD.

CS 3676-51

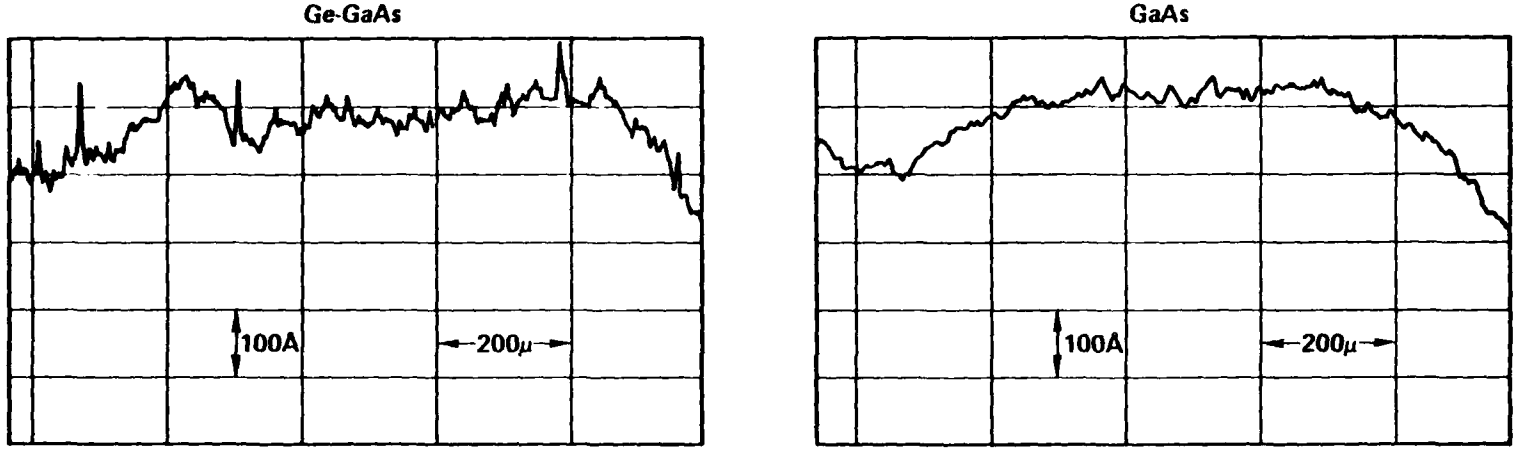

Fig. 3.16 DEKTAK measurements showing surface smoothness.

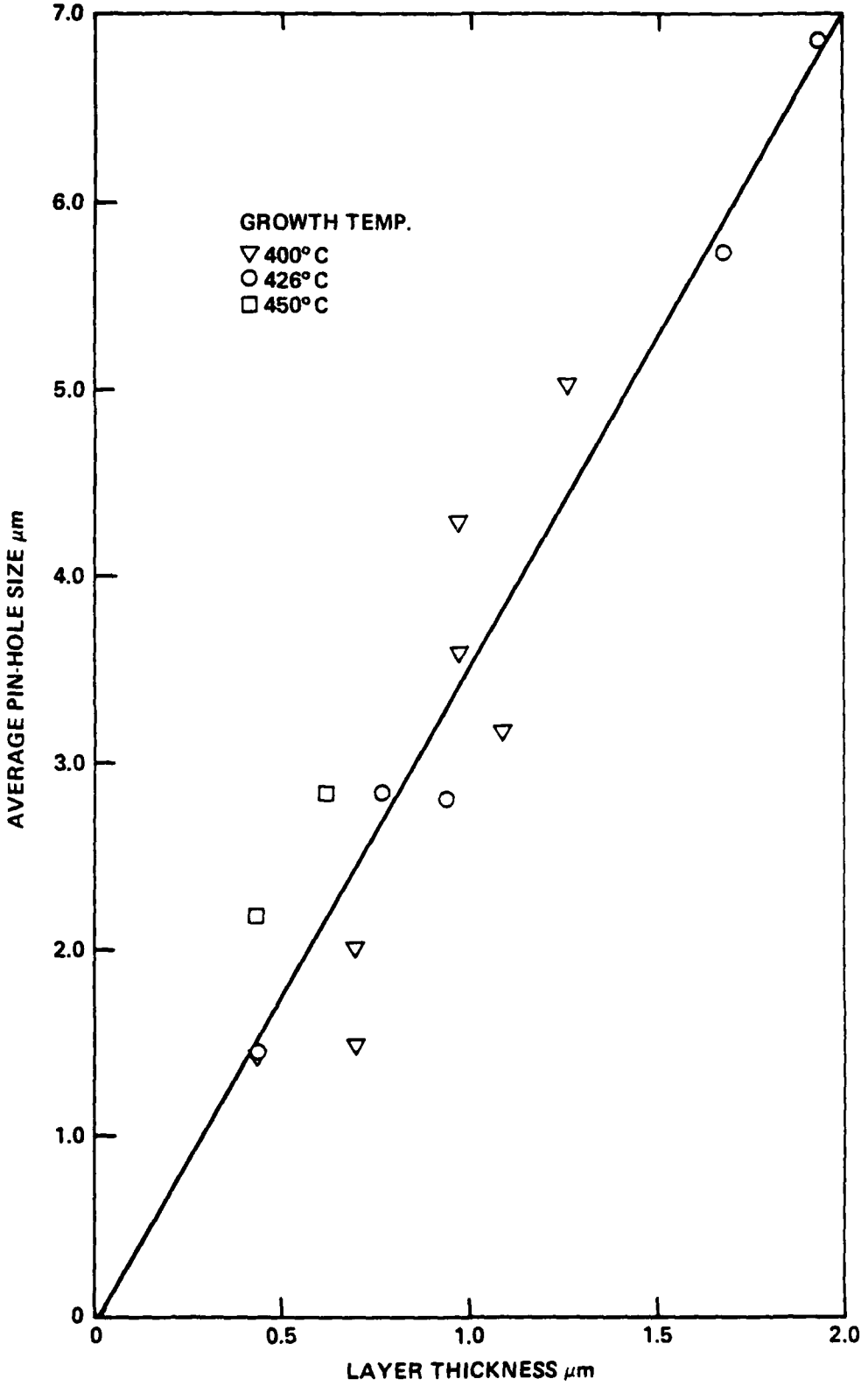

Fig. 3.17 Size of pinhole as a function of layer thickness.

interface was obtained on all three elements. A transition region of ~200Å was detected. This is shown in Fig. 3.18. When plotted on a log-linear plot, it can be seen that the interface is indeed sharp, with the Ga signal varied by four orders of magnitude within 200 A (Fig. 3.19). One thing to be pointed out here is that the carrier "pile-up" near the interface cannot be totally explained by the Ga or As coming out from the GaAs. A transition width of 200 A should be viewed as an upper limit, as the sputtering process does tend to roughen the surfaces causing some convolution of the actual profile. The background Ga signal in the Ge is probably due to noise and not Ga. Again, no extraneous impurities are detected from the Ge layers as shown by the 0-100 amu SIMS survey spectrum (Fig 3.20).

3.3.4 Growth Rate

Quite different from conventional vapor phase growth of epitaxial materials in which the growth is thermodynamically controlled and dependent on the free energy of reaction at the growth surface, plasma-enhanced CVD growth of Ge is primarily mass transport dependent. Other variables such as the rf power, the reactant concentration and the substrate temperature affects the growth rate to a lesser extent. The mechanism of the deposition of Ge from the PECVD is similar to that of evaporation in which deposition is uniform within the deposition zone, independent of the deposition surface. Substrate temperature mainly affects the crystallinity of the grown layer.

Our work so far demonstrates feasibility for submicron layer Ge growth. At a fixed temperature, the growth rate varies superlinearly with the

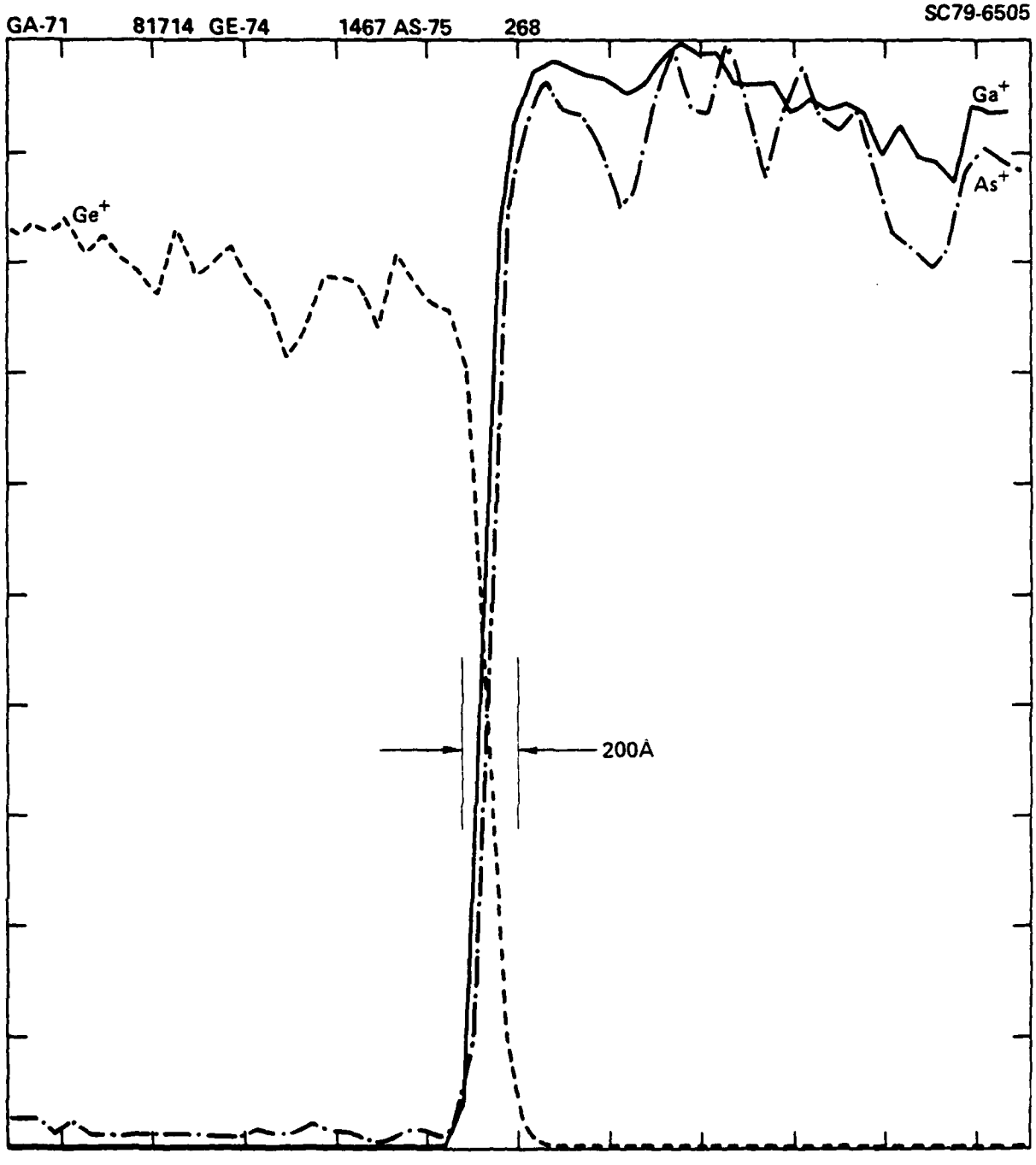

Fig. 3.18 SIMS plot showing Ge-GaAs junction.

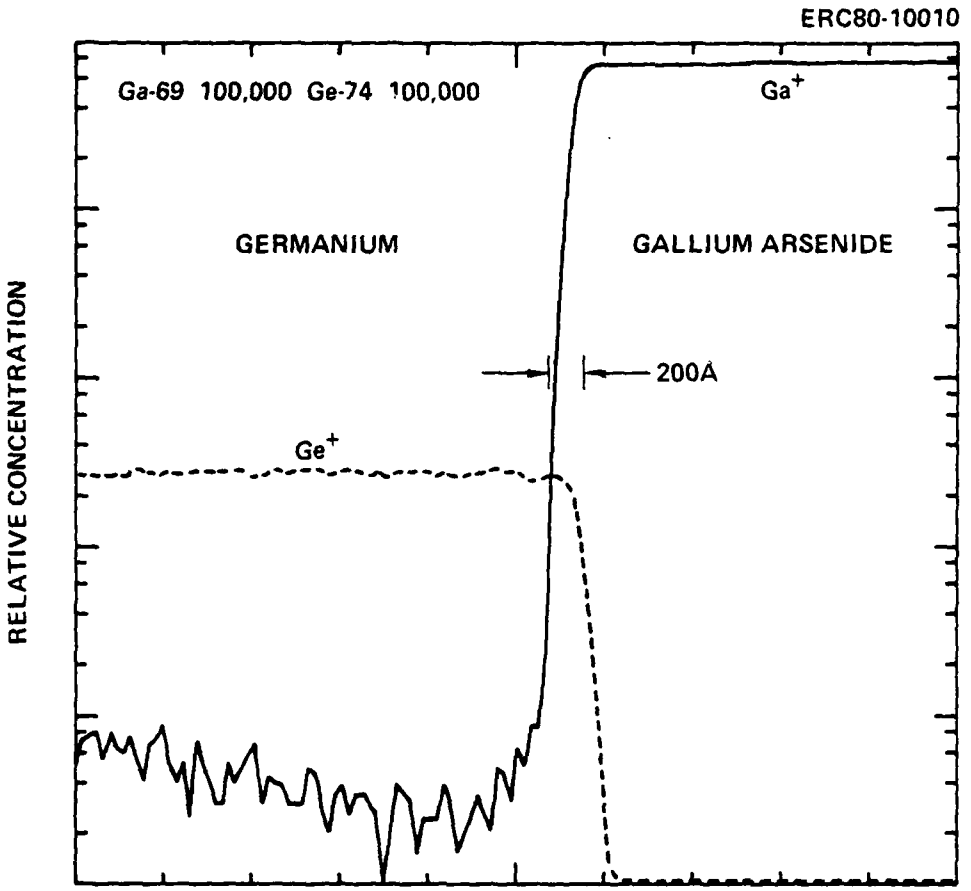

Fig. 3.19 Log-linear SIMS plot showing abruptness of Ge-GaAs junction.

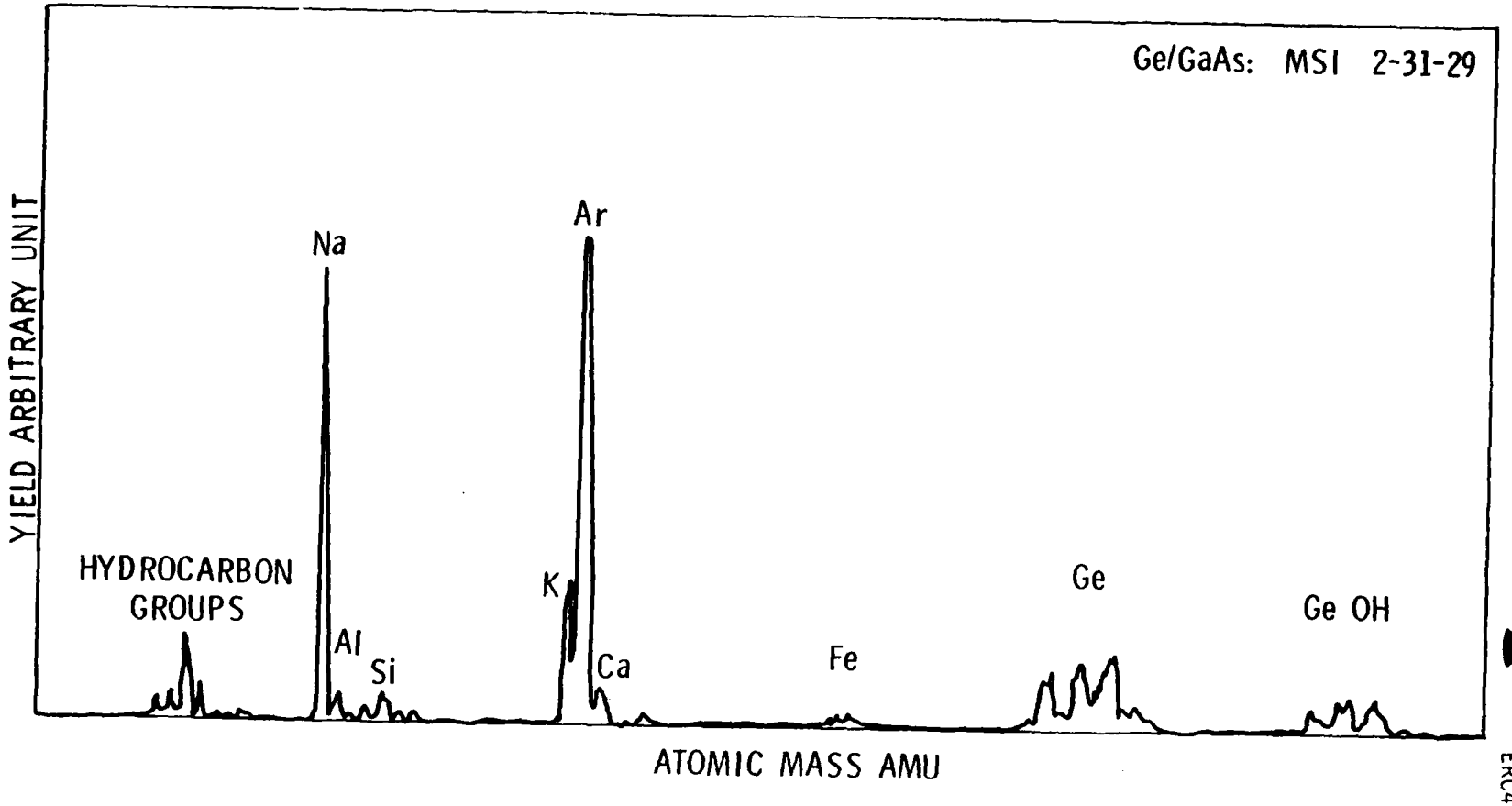

Fig. 3.20 SIMS survey spectrum showing various impurities.

flow rate. Therefore, by controlling the input flow rate which directly affects the linear flow velocity, controlled growth of Ge is achieved. Ge grown at 426°C are single crystalline, whereas those grown at 400°C exhibit amorphous regions as explained in Section 3.3.2.

It is also observed that the growth rate of the Ge affects the surface morphology of the Ge layers. The higher growth rate gave rise to pinholes which are undesirable, whereas the low growth rate gave a sputtered surface. The best growth condition, therefore, appears to be growing at 426°-450°C with a flow rate of ~40 sccm giving a growth-rate of ~0.5 μm/hr. This slow growth rate makes this PECVD a very attractive process to grow submicron layers.

3.3.5 Cold Wall Experiments

Cold wall experiment, in which the substrate was heated by the wire-wound heaters in the graphite susceptor, was performed. It was initially felt that by having a cold wall environment, purer material can be obtained because of reduced contamination from the furnace walls. It was found from later experiments that contaminations from the wall did affect the purity of the layer, especially for thin layers, but its effect was small compared to that due to the purity of the starting reactants, sputtering of the GaAs by the hydrogen plasma and defects near the interface. It was also found that layers grown by the cold wall method exhibited higher carrier concentration and lower mobility. This is probably due to an enhancement of structural defects in the layer.

In the hot wall process, the ions in the plasma have kinetic energy composed of the furnace thermal energy and the small energy that the electrons impart to the ions by elastic interaction. In the cold wall set-up, the ions in the plasma have only the small energy due to elastic interactions. Depending on the deposition rate of the germanium ions, they might not have picked up enough kinetic energy from the hot substrate to move around on the substrate for a suitable site before they were caused immobile by incoming ions. Insufficient kinetic energy of the incoming ions might cause insufficient mobility of the ions which in turn gave rise to defect growth due to stacking faults. In view of the fact that the cold wall growths did not result in an improvement in the purity of the layers, the hot wall process was used in subsequent runs so that a meaningful comparison between different doping experiments, gas mixtures and substrate cleaning experiments can be made.

3.3.6 Plasma Cleaning

In situ plasma cleaning of the substrate before growth was performed to investigate its effect on the purity of the layer. Plasma cleaning of reactor components in situ between depositions was also evaluated. Results of these plasma cleaning are summarized below.

Hydrogen plasma was used to clean the hot GaAs substrates prior to the Ge epitaxial growth. Various rf power levels and plasma durations of a few seconds to a few minutes were tried. Afterwards epitaxial Ge were grown on the semi-insulating GaAs as described previously. The purity of the grown

layers were then investigated. The results are shown in Fig. 3.21. Also plotted in Fig. 3.21 are the results of layers grown without hydrogen plasma cleaning. It is clear from the results that the hydrogen plasma raised the background impurities concentration by a factor of ~ 3. No improvement in the distribution of the interface charges is seen.

Next, plasma cleaning with CF_4 was tried. CF_4 was used in plasma etching of Si, Ge and SiO_2, as well as in plasma ashing of photoresists. Our results showed that CF_4 plasma can be used to clean the reactor components (i.e., the liner tube as well as the susceptors), however, the rate of Ge removal is very slow. When GaAs substrate was subjected to the CF_4 plasma, a very thin layer of carbon was found on the surface of the GaAs. Subsequent Ge growth on these layers gave unsatisfactory results, yielding amorphous layers or layers that did not stick to the GaAs at all. In view of these results, vacuum baking prior to growth was preferred over plasma cleaning for removing the oxides on the GaAs substrates. Further work needs to be done to obtain a satisfactory plasma cleaning process for GaAs.

3.3.7 Doped Layers

Intentional doping using B_2H_6 has been carried out on Ge layers grown on semi-insulating GaAs substrates and GaAs epitaxial active layers. Up to 200 sccm flow of 5 ppm B_2H_6 in UHP H_2 was used. Hot point probe indicated that the layers were p-type but Van der Pauw results indicated they were n-type. This can be understood by assuming that the B_2H_6 compensated the layers but not enough to compensate for the huge carrier "pile-up" near the

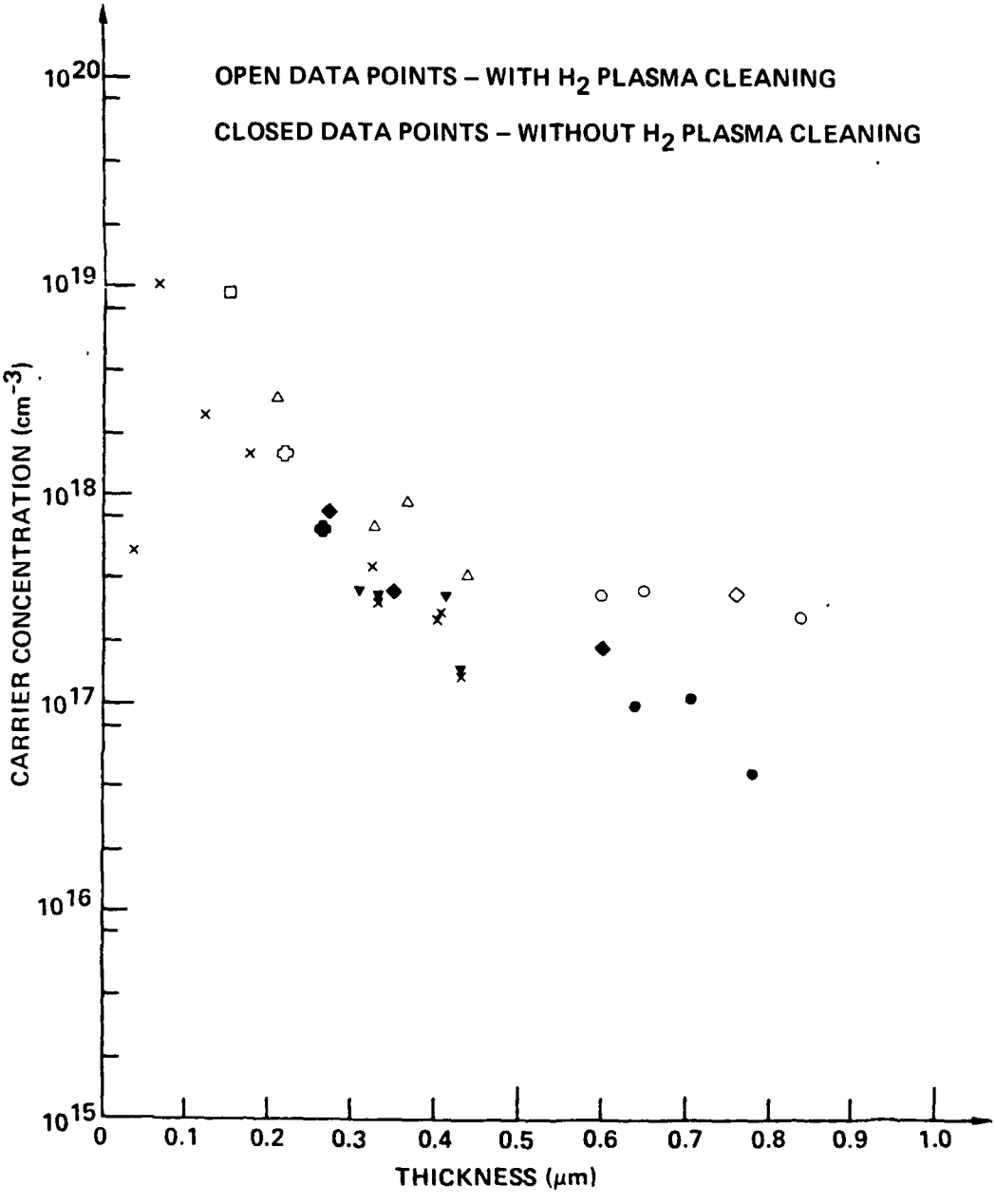

Fig. 3.21 <n> vs thickness of layers grown using PECVD with and without H_2 plasma cleaning.

interface. This resulted in layers having high n-type carriers near the interface but p-type region near the surface. Because of this, the Van der Pauw as well as the differential VDP data for these layers are unreliable. Hot point probe generated holes near the surface whereas the Van der Pauw technique detected the heavier electron concentration near the interface. Doping using B_2H_6 is obviously effective but more work needs to be performed on the control of the interface charges before a reliable back-doping process can be established.

The doping concentration of the Ge layer can be estimated by assuming that both the GeH_4 and B_2H_6 have the same ionization rates and deposition rates. The ionization of every GeH_4 molecule gives one Ge ion, whereas that of B_2H_6 gives two B ions. Therefore, the ratio of boron ions to germanium ions is given by:

$$R = \frac{\text{Flow } (B_2H_6)}{\text{Flow } (GeH_4)} \times 2$$

$$= \frac{\text{Flow } (B_2H_6/H_2 \text{ Mix})}{\text{Flow } (GeH_4/H_2 \text{ Mix})} \times \frac{\text{Conc. } B_2H_6 \text{ in } H_2}{\text{Conc. } GeH_4 \text{ in } H_2} \times 2$$

and the concentration of boron in the deposited germanium is then equal to:

$$[B] = R \times \frac{\text{Density (Ge)}}{\text{Mol. wt. (Ge)}} \times \text{Avogadros No.}$$

With equal flow (100 sccm) of 5 ppm B_2H_6 and 1% GeH_4 mixtures, [B] is calculated to be $\sim 4.4 \times 10^{19}$ cm^{-3}. This is in excellent agreement with that

obtained from 4-point probe measurements on layers grown on Ge substrates giving $\rho \sim 9 \times 10^{-4}$ Ω-cm or $p \sim 4 \times 10^{19}$ cm^{-3}.

Intentional in situ Ge p-n junction growths have also been performed. (100) Sb-doped Ge substrates with $\rho \sim 0.01$-0.04 Ω-cm were used. A layer of n-type Ge ~ 0.8 μm thick was first grown on the Ge substrate after which 100 sccm of 5 ppm B_2H_6 was introduced into the growth chamber, and another ~ 0.8 μm thick boron-doped Ge was grown. This resulted in a p-type Ge with $\rho \sim 0.001$ Ω-cm as determined from 4-point probe measurement. Metal contacts were evaporated on the front and back side and mesas were etched. Electrical measurements of these junction are reported in the next section.

3.3.8 Electrical Measurements

In order to assess the electrical nature of the heterojunction interface, Ge-GaAs heterojunctions are fabricated and the results are reported here. Gallium arsenide and Ge epitaxial layers were grown in two separate runs, with GaAs epi grown by LPE or VPE and Ge grown by PECVD at ~ 450°C. (100) oriented n^+ GaAs substrates were used. Evaporated 10 mil dia. Ti-Au dots were defined on the Ge by shadow masking, after which mesas were etched with warm 5:1:1:H_2SO_4:H_2O:H_2O_2. This etch removes both the Ge and GaAs. Standard Au-Ge alloy was used for ohmic contact to the n^+ GaAs.

Three types of heterojunction structures were studied, they are listed in the following table.

Table 3.1

Various Ge-GaAs Heterojunctions Investigated

	Ge	GaAs Epitaxial Layer	GaAs Substrate
I	$p \sim 10^{17}$ cm^{-3}		n^+
II	$p \sim 10^{17}$ cm^{-3}	$n \sim 10^{16}$ cm^{-3} LPE grown	n^+
III	$n \sim 7 \times 10^{17}$ cm^{-3}	$n \sim 2 \times 10^{16}$ cm^{-3} VPE grown	n^+

The I-V characteristics for the above cases are shown in Figs. 3.22 to 3.28. With the p-Ge grown on n^+ GaAs substrate, it exhibited soft reverse breakdown at low voltages (Fig. 3.22). In the forward direction, $V_f \cong 0.22$ V when $I_f = 1$ mA (Fig. 3.23). When the forward current was plotted against forward voltage and the data fitted to the ideal diode equation (Eq. (2.1)), the ideality factors were calculated to be 1.9 at room temperature and 7.7 at 77K (Fig. 3.24). This strong temperature dependence of n is characteristic of a tunnel junction and in fact is expected for a junction between a $p \sim 10^{17}$ cm^{-3} Ge and n^+ GaAs. In fact, the above I-V data can be replotted using the ideal tunnel junction diode law

$$I = I_0 [\exp (AV) - 1] \qquad (3.1)$$

giving $A \cong 20$ V^{-1}, approximately independent of temperature. I_0 dopped by two orders of magnitude when T decreases from 300K to 77K. When $p \sim 10^{17}$ cm^{-3} Ge was grown on $n \sim 10^{16}$ cm^{-3} GaAs, a different situation arose as expected (Fig. 3.25).

SC79-6387

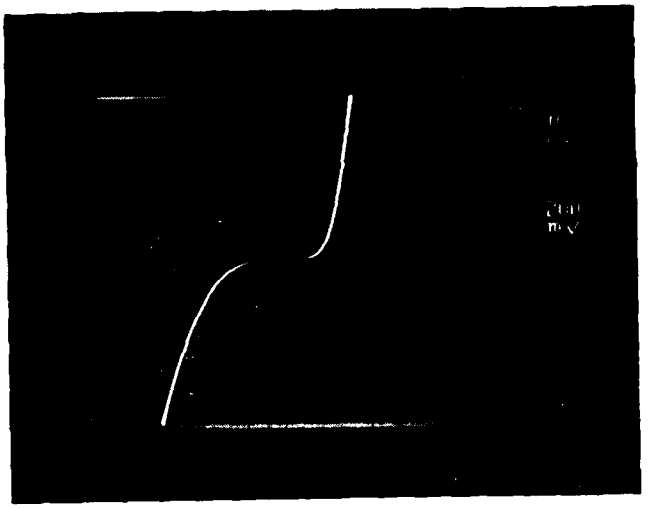

Fig. 3.22 I-V characteristics of a p 10^{17} Ge on n^+ GaAs.

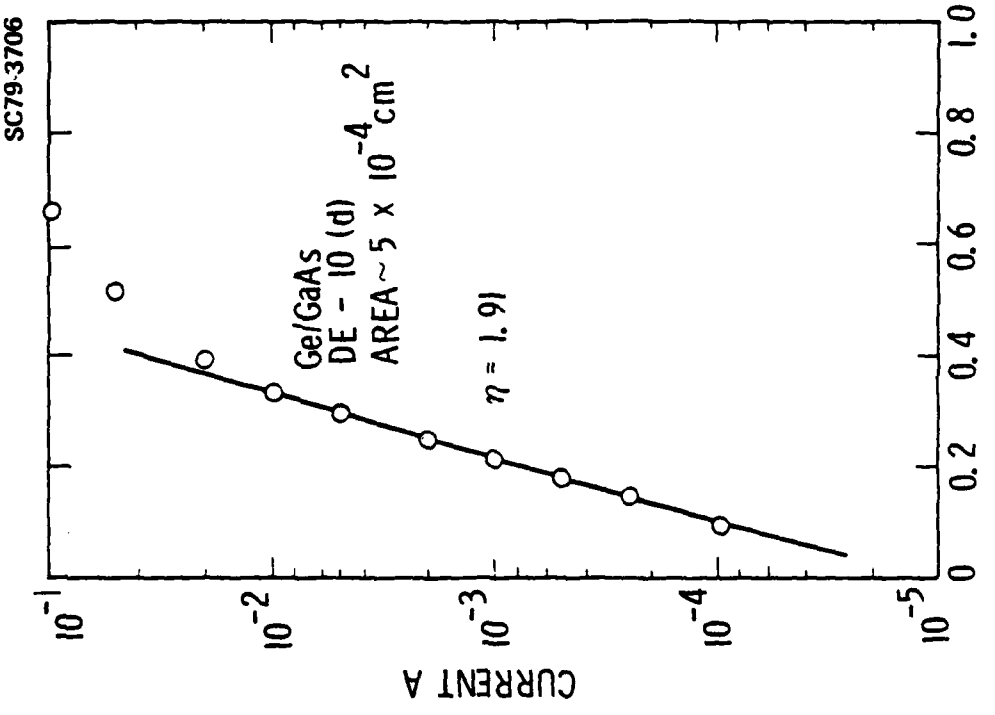

Fig. 3.23 Log-linear plot of forward I-V characteristics of p Ge-n^+ GaAs heterojunction at room temperature.

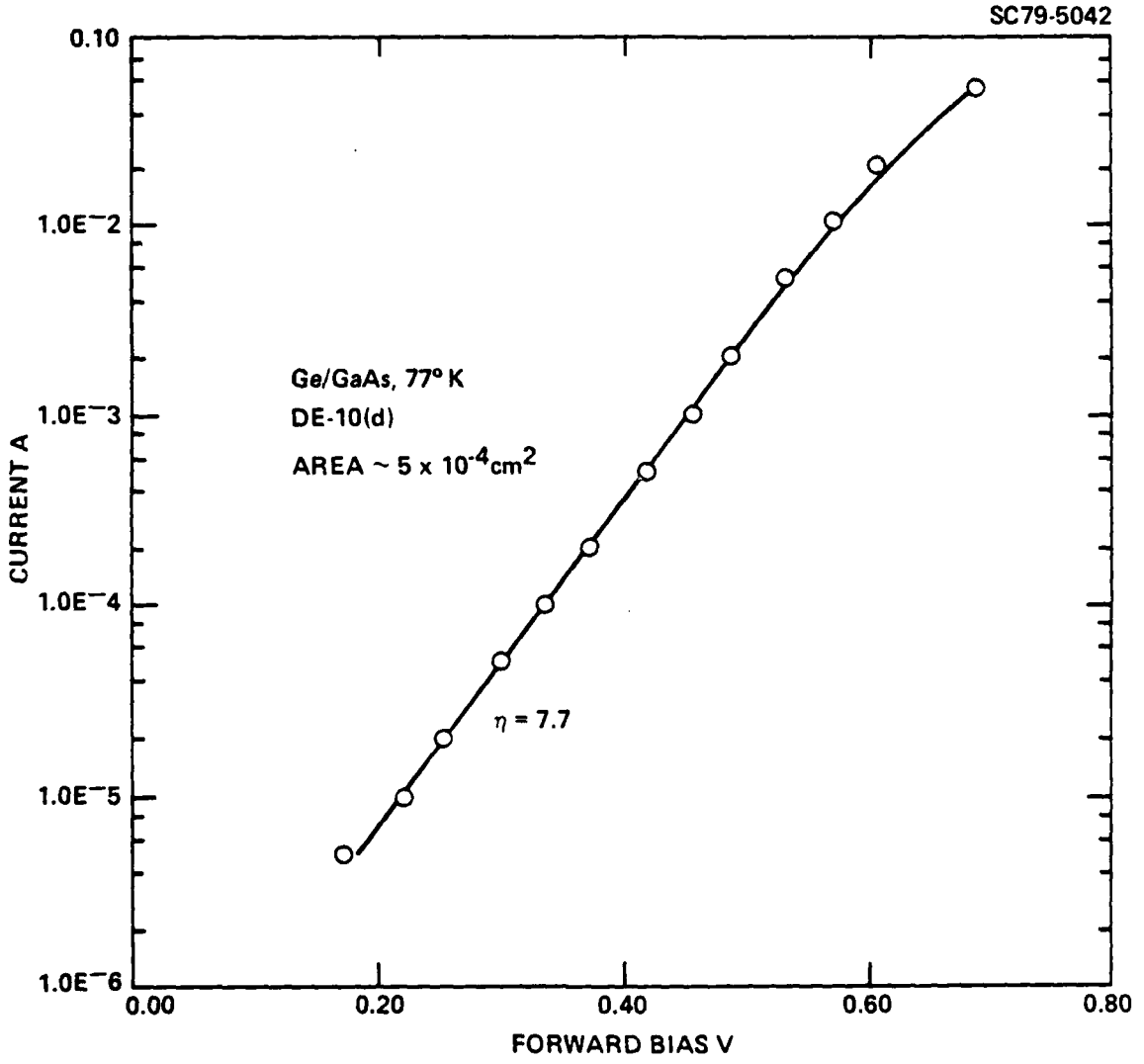

Fig. 3.24 Log-linear plot of forward I-V characteristics of p-Ge-n^+ GaAs heterojunction at 77K.

SC79-5956

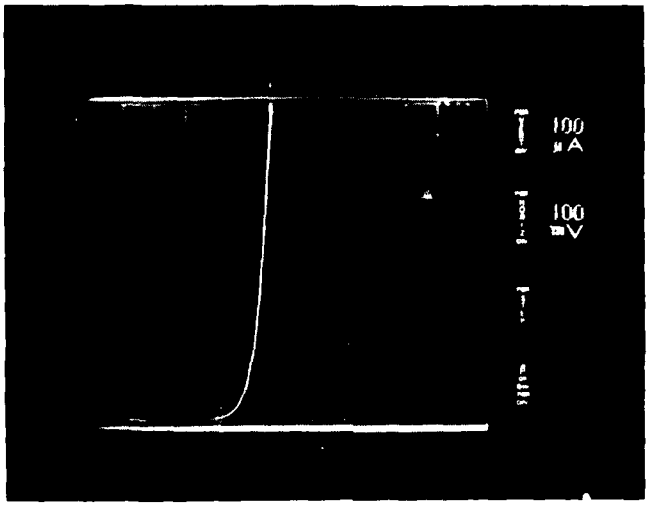

(a)

170F8ST-1

SC79-5039

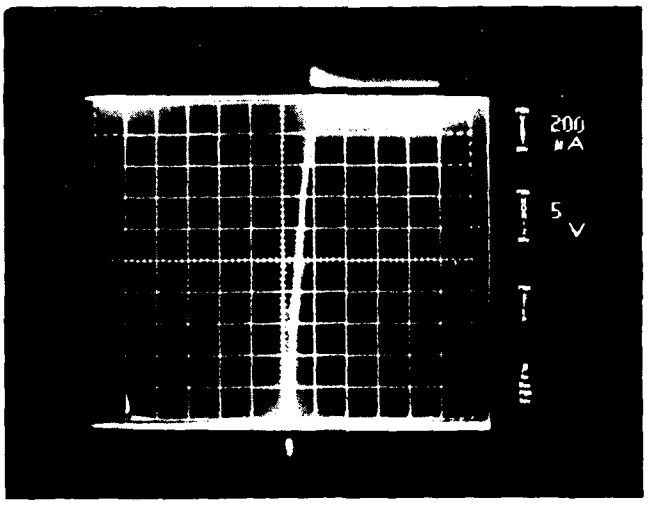

(b)

Fig. 3.25 (a) Forward I-V characteristic of a p ~ 10^{17} Ge on n ~ 10^{16} GaAs.
(b) Reverse I-V characteristics of a p ~ 10^{17} Ge on n ~ 10^{16} GaAs.

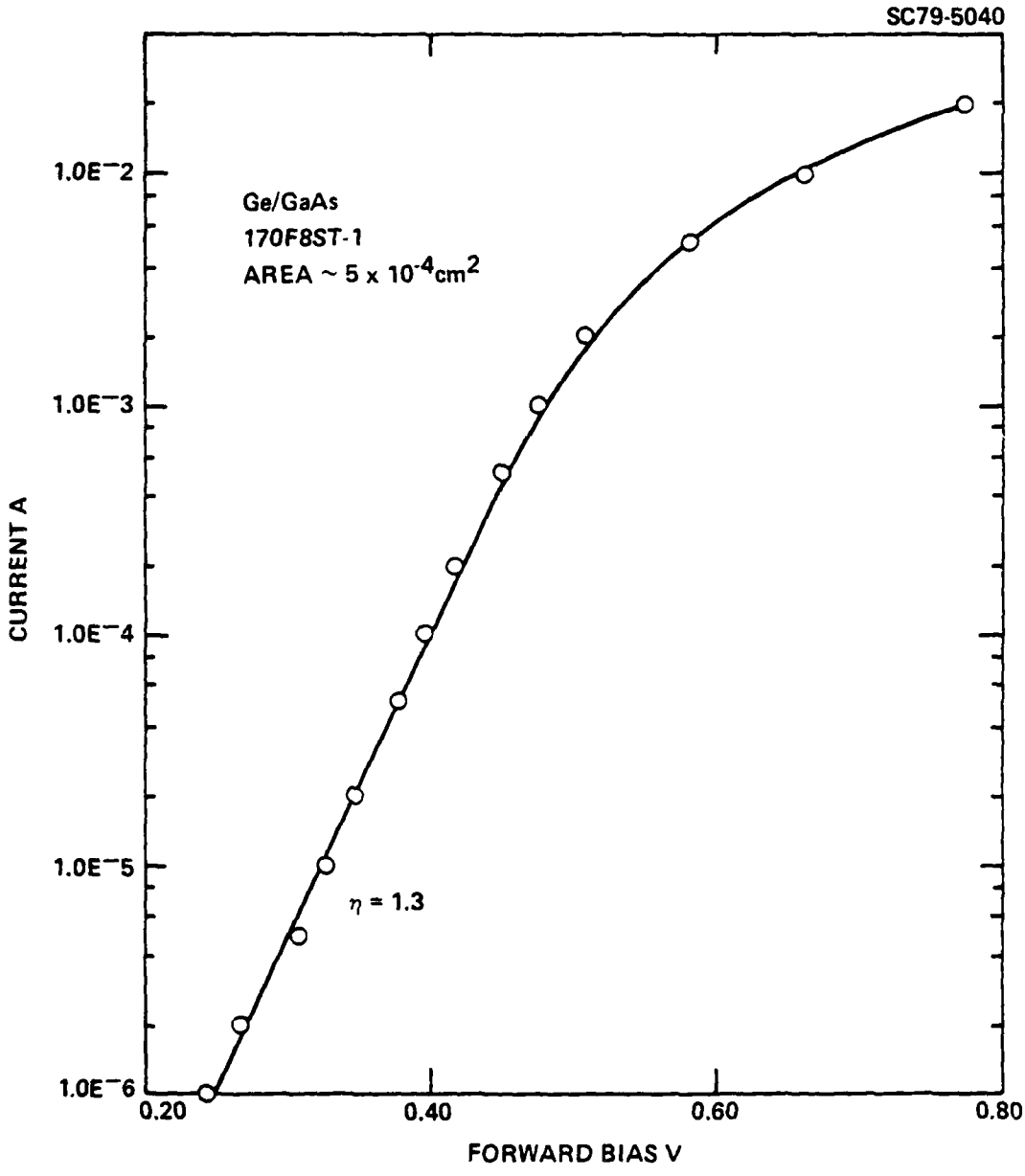

Fig. 3.26 Log-linear plot of forward I-V characteristics of p Ge-n GaAs heterojunction at room temperature.

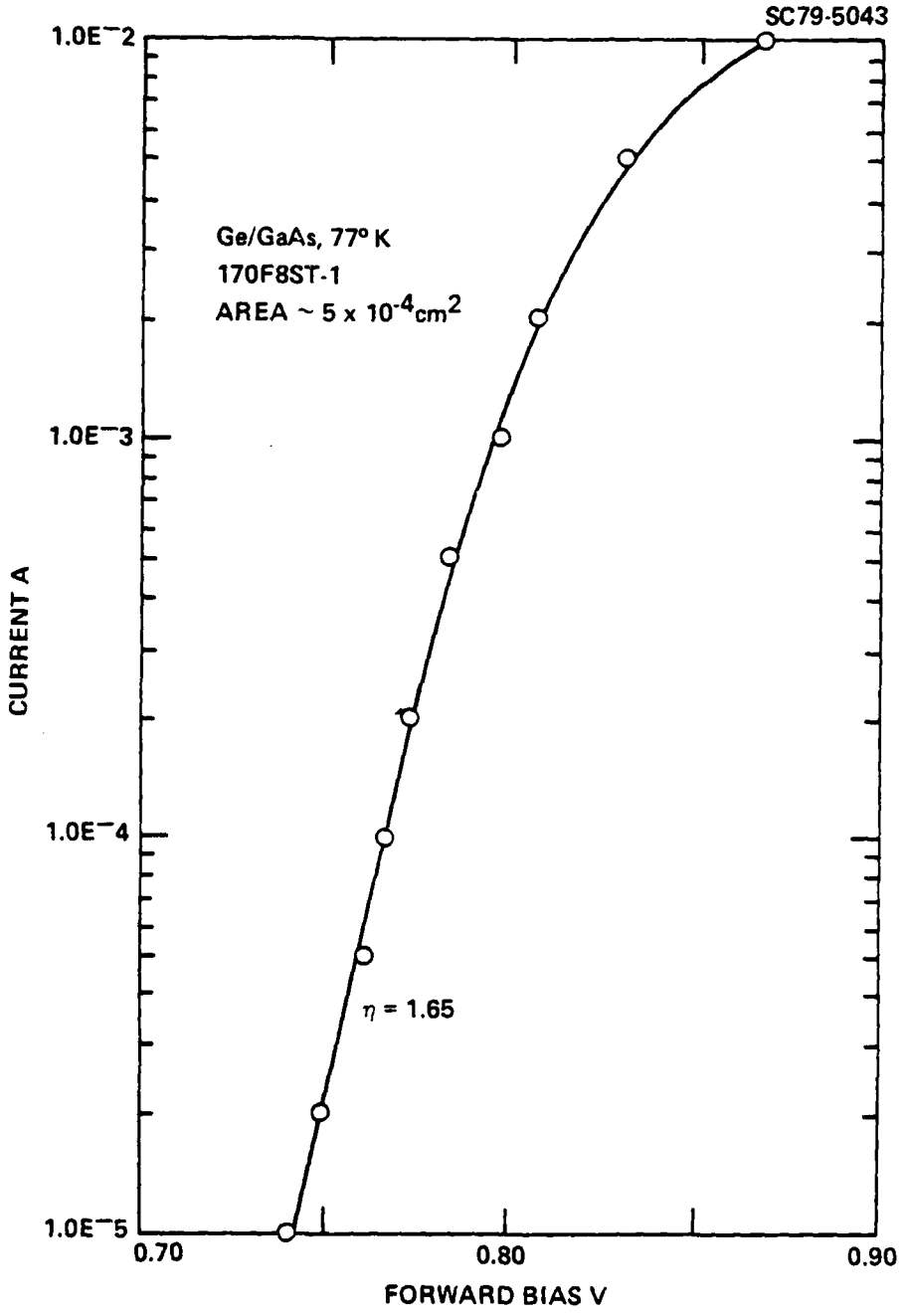

Fig. 3.27 Log-linear plot of forward I-V characteristics of p Ge-n GaAs heterojunction at 77K.

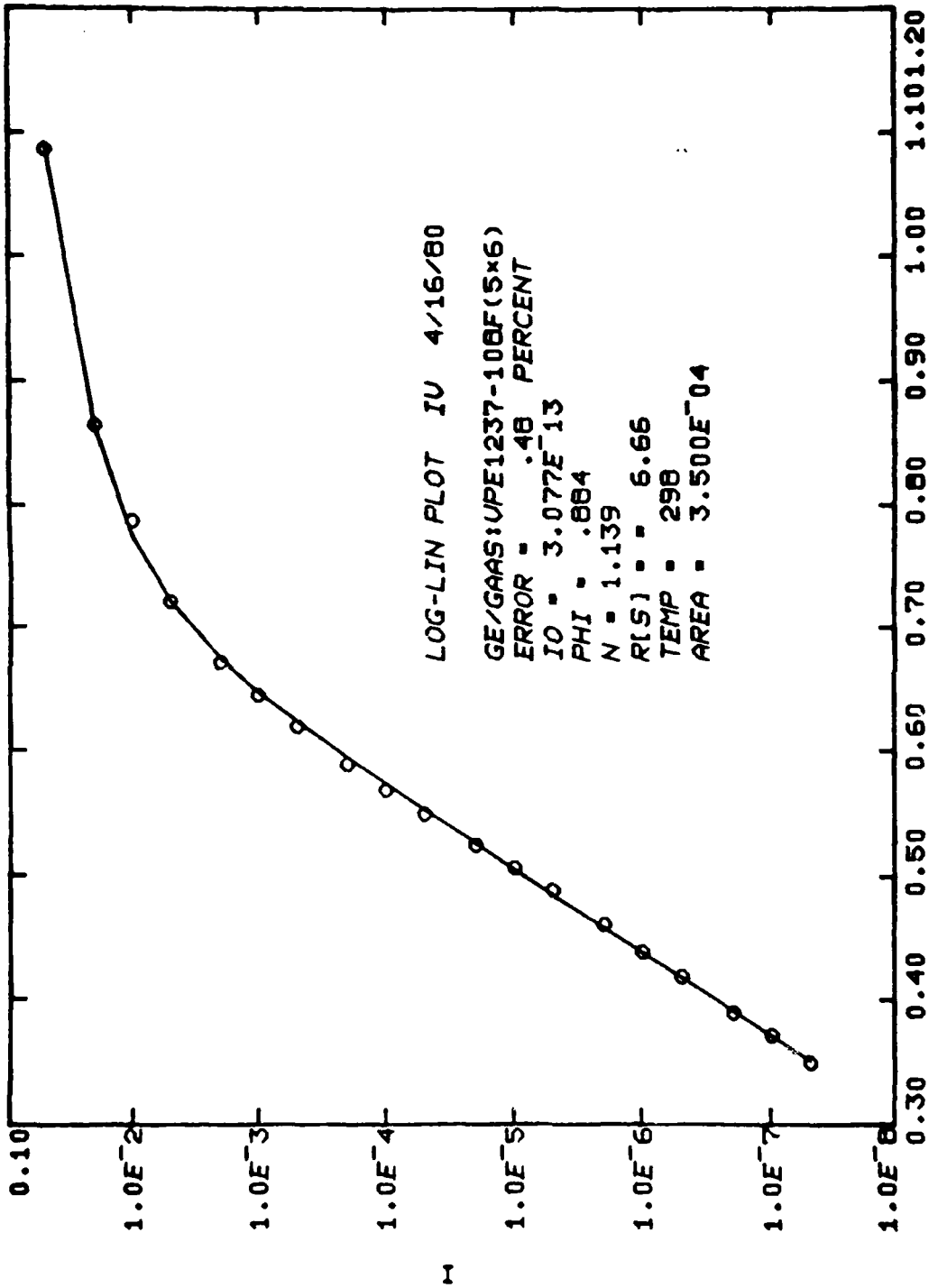

Fig. 3.28 Log-linear plot of forward I-V characteristics of n Ge-n GaAs at room temperature.

The I-V characteristics are shown in Fig. 3.26 showing a forward voltage of ~ 0.48 V for I_f = 1 mA and a sharp reverse breakdown voltage of about 20 V. The reverse bias current is small, on the order of a nA. The ideality factors at room temperature and 77K are 1.3 and 1.65 respectively. It is seen from Fig. 3.27 that at 77K no appreciable current was flowing until V_f > 0.7 V. This indicated a substantial barrier was formed in the p-n heterojunction at 77K.

For the n-n heterojunction, room temperature I-V measurements shown in Fig. 3.28 showed that this junction appeared to behave very much like a Schottky diode on GaAs with ϕ = 0.88 V, and $n \approx 1.14$. The fit of the data to the ideal diode equation was excellent with an error of ~ 0.48%. The reverse breakdown was sharp with a breakdown voltage of ~ 40 V. With an electron concentration of ~ 2×10^{15} cm^{-3}, a GaAs Schottky barrier diode would have a breakdown voltage of ~ 100 V. This lower breakdown voltage in the Ge-GaAs diode indicated that it is the germanium that is breaking down. Further examination will be performed on these diodes to locate the position of the junction.

In situ germanium p^+-n junctions were also grown on n-type germanium substrates. Forward I-V characteristics of diodes from two different layers are shown in Fig. 3.29. $n \sim 1$ is obtained for the diodes. In the reverse bias situation, the breakdown is very soft, with a breakdown voltage < 2 V. This is expected because both the n and p epilayers have carrier concentration > 10^{17} cm^{-3}.

AD-A102 889 ROCKWELL INTERNATIONAL THOUSAND OAKS CA ELECTRONICS--ETC F/G 20/2
EPITAXIAL GROWTH OF GE0AAS.(U)
JUN 81 K T IP, R D FAIRMAN, A A IMMORLICA F44620-76-C-0134
UNCLASSIFIED ERC41002.29FR AFOSR-TR-81-0632 NL

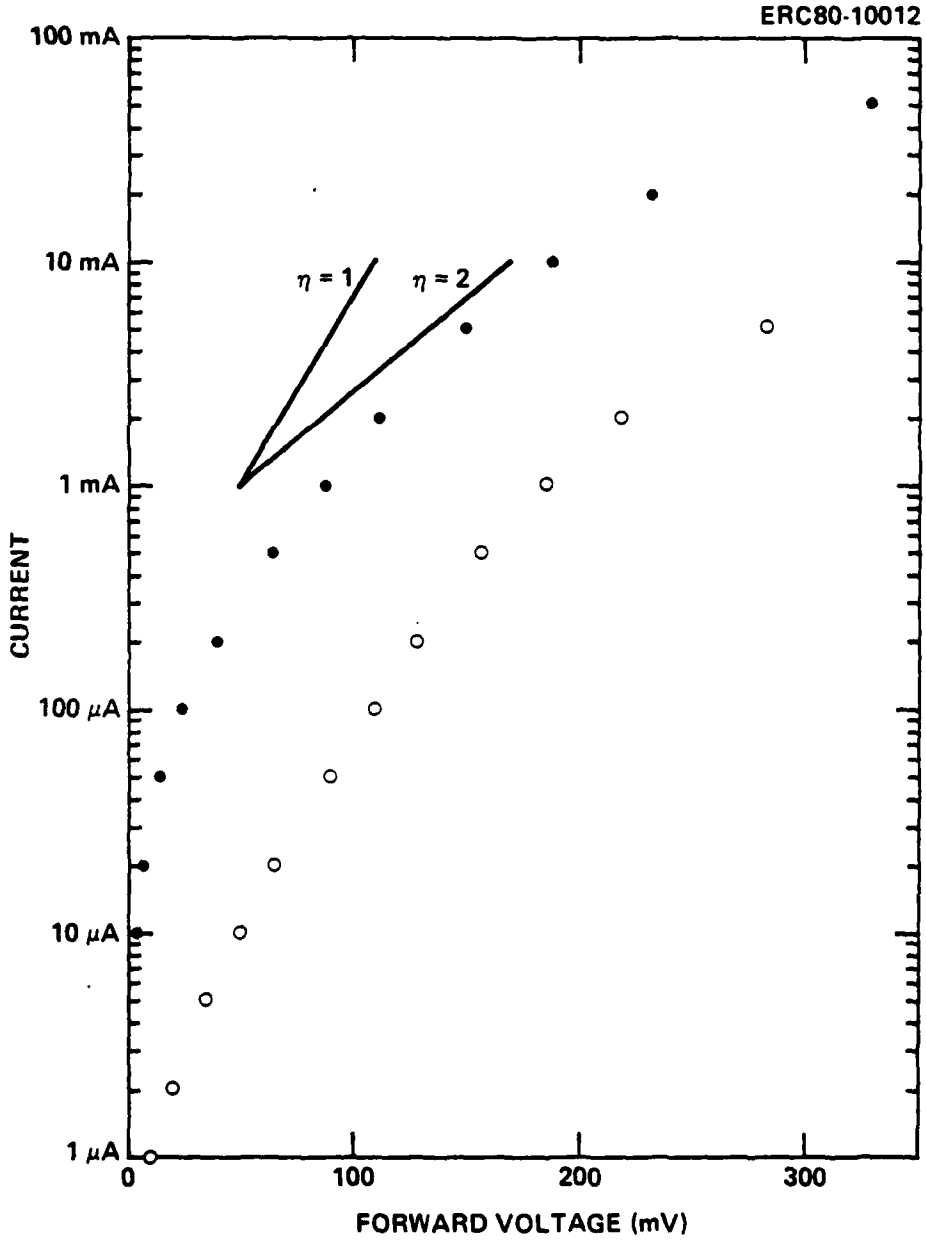

Fig. 3.29 Log-linear plot of forward I-V characteristics of two Ge p-n junctions grown by PECVD.

4.0 SUMMARY AND RECOMMENDATIONS

The work performed in this program has significantly improved the technique of growing Ge on GaAs. Using the LPE technique, fairly heavily doped Ge layers were obtained because of thermodynamic instability at the melt-seed interface. The purity of the Ge layers was greatly improved by using the Plasma-Enhanced CVD technique. p-type layers with $p \sim 1 \times 10^{16}$ cm^{-3} and $\mu_p \sim 1500$ $cm^2/V\text{-}s$ have been achieved. Mirror smooth layers with sharp interfaces are routinely obtained. Doping with volatile hydride is now possible and indeed compatible with the PECVD technique. Up to $p \sim 10^{19}$ cm^{-3} has been obtained in layers intentionally doped with B_2H_6. In situ growth of multi-layer structures has also been demonstrated.

The results show some carrier "pile-up" near the Ge-GaAs interface. Additional study of this interface charge would prove to be very fruitful and would enhance the physical understanding of a polar- nonpolar heterojunction. Nevertheless the PECVD growth technique for Ge on GaAs has progressed to the stage where a renewed investigation of this heterojunction system for microwave device applications is strongly recommended.

The successful growth of Ge on GaAs using PECVD demonstrated that it is possible to grow epitaxial layers where the main energy for the reaction is derived not from thermal energy, but from the plasma energies of the electrons. This opens up a new way of growing epitaxial materials that was previously prohibited because of thermal limitations. By the addition of a plasma, a number of formerly impossible reactions are now possible. Examples

are some III-V and II-VI semiconducting materials that require a low substrate temperature but a high reaction temperature; specific examples are GaP, InP and HgCdTe. It is therefore recommended that the growth of other semiconducting materials, using the PECVD technique and progressing from III-V compounds to ternary and quaternary compounds and extending to II-VI compounds, be investigated.

5.0 REFERENCES

1. J. R. Arthur, J. Physics and Chemistry of Solids 28, 2257 (1967).
2. A. Laugier, Ph.D. Thesis, University of Lyon, France (1964).
3. H. Nelson, RCA Review 24, 603 (1963).
4. S. M. Sze, Physics of Semiconductor Devices, Wiley, New York, 1969.
5. A. C. Milnes, Deep Impurities in Semiconductors, Wiley, New York, 1973.
6. J. C. Brice, The Growth of Crystals from Liquids, American Elsevier, New York, 1973.
7. O. Wells, Scanning Electron Microscopy, McGraw Hill, New York, 1974.
8. C. M. Garner, Y. D. Shen, T. S. Kim, G. L. Pearson, W. E. Spicer, J. S. Harris, Jr., and D. D. Edwall, J. Applied Phys. 48, 3147 (1977).
9. Honig, RCA Review 23, 567 (1962).
10. B. W. Sloope and C. O. Tiller, J. Appl. Phys. 38, 140 (1967).
11. J. R. Hollahan and A. T. Bell, Techniques and Applications of Plasma Chemistry, Wiley, N. Y., 1974.
12. H. Dricer, Phys. Rev. 117, 343 (1960).
13. N. Neuert, et al., Z. Naturforsch 7a, 410 (1952).
14. F. Glocking, The Chemistry of Germanium, Academic Press, N. Y., 1969.
15. C. T. Toxon, J. A. Harvey and B. A. Joyce, J. Phys. Chem. Solids 34, 1693 (1973).
16. J. R. Arthur, J. Phys. Chem. Solids 28, 2257 (1967).
17. A. Y. Cho and F. K. Reinhart, J. Appl. Phys. 45, 1812 (1974).

18. J. B. Light, M. Berkenblit and A. Reisman, J. Electrochem. Soc. 115, 969 (1968).

19. K. T. Ip and R. D. Fairman, "Plasma Enhanced Epitaxy of Ge on GaAs," presented at WOCSEMMAD, Atlanta, Ga, Feb. 1979.

20. K. T. Ip and R. D. Fairman, "Epitaxial Growth of Ge on GaAs by Plasma-Enhanced CVD," presented at Electronics Materials Conference, Boulder, Colorado, June 1979.

21. T. Itoh, et al., "The Silicon Epitaxial Growth by the Plasma Dissociation of Silane," presented at the Electrochemical Society Meeting, Pittsburgh, Pa. Oct. 1978.

22. J. E. Davey, Appl. Phys. Lett. 8, 164 (1966).

23. C. Wood, private communication.

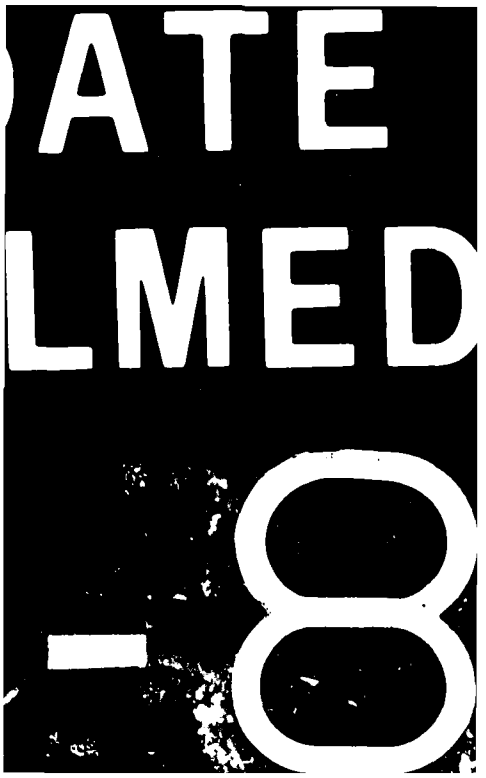
ATE
LMED
-8